



Dissanayake, P. D. et al. (2020) Biochar-based adsorbents for carbon dioxide capture: a critical review. *Renewable and Sustainable Energy Reviews*, 119, 109582. (doi: [10.1016/j.rser.2019.109582](https://doi.org/10.1016/j.rser.2019.109582))

The material cannot be used for any other purpose without further permission of the publisher and is for private use only.

There may be differences between this version and the published version. You are advised to consult the publisher's version if you wish to cite from it.

<http://eprints.gla.ac.uk/202958/>

Deposited on 11 November 2019

Enlighten – Research publications by members of the University of
Glasgow

<http://eprints.gla.ac.uk>

Biochar-based adsorbents for carbon dioxide capture: A critical review

Pavani Dulanja Dissanayake^{a,i,#}, Siming You^{b,#}, Avanthi Deshani Igalavithana^a, Yinfeng Xia^c,
Amit Bhatnagar^d, Souradeep Gupta^e, Harn Wei Kua^e, Sumin Kim^f, Jung-Hwan Kwon^g, Daniel
C.W. Tsang^{h,**}, and Yong Sik Ok^{a,*}

^aKorea Biochar Research Center, O-Jeong Eco-Resilience Institute & Division of
Environmental Science and Ecological Engineering, Korea University, Seoul 02841, Korea

^bSchool of Engineering, University of Glasgow, Glasgow, UK

^cCollege of Water Conservancy and Environmental Engineering, Zhejiang University of
Water Resources and Electric Power, Hangzhou 310018, People's Republic of China

^dDepartment of Environmental and Biological Sciences, University of Eastern Finland, P.O.
Box 1627, FI-70211 Kuopio, Finland

^eDepartment of Building, School of Design and Environment, National University of
Singapore, 4 Architecture Drive, S117566, Singapore

^fDepartment of Architecture and Architectural Engineering, Yonsei University, Seoul 03722,
Korea

^gDivision of Environmental Science and Ecological Engineering, Korea University, Seoul
02841, Korea

^hDepartment of Civil and Environmental Engineering, Hong Kong Polytechnic University,
Hung Hom, Kowloon, Hong Kong

ⁱSoils and Plant Nutrition Division, Coconut research Institute, Lunuwila 61150, Sri Lanka

[#]The authors contributed equally to the paper

*Corresponding Author:

Email address: yongsikok@korea.ac.kr

**Co-corresponding Author:

Email address: dan.tsang@polyu.edu.hk

28 **Abstract**

29 Carbon dioxide (CO₂) is the main anthropogenic greenhouse gas contributing to global
30 warming, causing tremendous impacts on the global ecosystem. Fossil fuel combustion is the
31 main anthropogenic source of CO₂ emissions. Biochar, a porous carbonaceous material
32 produced through the thermochemical conversion of organic materials in oxygen-depleted
33 conditions, is emerging as a cost-effective green sorbent to maintain environmental quality by
34 capturing CO₂. Currently, the modification of biochar using different physico-chemical
35 processes, as well as the synthesis of biochar composites to enhance the contaminant sorption
36 capacity, has drawn significant interest from the scientific community, which could also be
37 used for capturing CO₂. This review summarizes and evaluates the potential of using pristine
38 and engineered biochar as CO₂ capturing media, as well as the factors influencing the CO₂
39 adsorption capacity of biochar and issues related to the synthesis of biochar-based CO₂
40 adsorbents. The CO₂ adsorption capacity of biochar is greatly governed by physico-chemical
41 properties of biochar such as specific surface area, microporosity, aromaticity,
42 hydrophobicity and the presence of basic functional groups which are influenced by
43 feedstock type and production conditions of biochar. Micropore area ($R^2 = 0.9032$, $n=32$) and
44 micropore volume ($R^2 = 0.8793$, $n=32$) showed a significant positive relationship with CO₂
45 adsorption capacity of biochar. These properties of biochar are closely related to the type of
46 feedstock and the thermochemical conditions of biochar production. Engineered biochar
47 significantly increases CO₂ adsorption capacity of pristine biochar due to modification of
48 surface properties. Despite the progress in biochar development, further studies should be
49 conducted to develop cost-effective, sustainable biochar-based composites for use in large-
50 scale CO₂ capture.

1
2
3
4
5
6
7
8
9
10
11
12
13
14
15
16
17
18
19
20
21
22
23
24
25
26
27
28
29
30
31
32
33
34
35
36
37
38
39
40
41
42
43
44
45
46
47
48
49
50
51
52
53
54
55
56
57
58
59
60
61
62
63
64
65

Highlights

- Engineered biochar possesses significantly high CO₂ adsorption capacity.
- Basic functional groups and hetero atoms are important for high CO₂ adsorption capacities.
- New technologies are needed for regenerating and reusing captured CO₂.

Keywords: black carbon; CO₂ capture; climate change; engineered biochar; greenhouse gas

Word Count: 7,781

77 1. Introduction

78 Global warming caused by the anthropogenic emission of greenhouse gases such as
79 carbon dioxide (CO₂), methane (CH₄), and nitrous oxide (N₂O) has become a serious
80 environmental issue in the last few decades [1]. It has been reported that CO₂ is the main
81 greenhouse gas responsible for global warming [2]. Since 1750, the atmospheric CO₂
82 concentration has increased reaching a level of 410 ppm at present [2]. The International
83 Panel on Climate Change (IPCC) has predicted that the CO₂ concentration will reach 570
84 ppm by 2100, leading to a mean temperature increase of 1.9 °C [3]. This would have a
85 tremendous impact on the terrestrial environment, causing heavy droughts, changes in rainfall
86 patterns, extreme heat waves, melting of glaciers, and rising sea levels [4]. Thus, it is
87 essential to develop sustainable methods for capturing and storing CO₂ to reduce CO₂
88 emissions and combat global warming, as underlined by the fifth assessment report of the
89 IPCC [3].

90 CO₂ capture technologies can be categorized into three groups: pre-combustion CO₂
91 capture, post-combustion CO₂ capture, and oxy-fuel combustion [5]. In pre-combustion CO₂
92 capture, H₂ and CO₂ are produced through the gasification of fossil fuel in a water-gas-shift
93 reactor, and H₂ is used for energy generation, whereas CO₂ is captured before the combustion
94 of the fossil fuel [4]. During post-combustion, CO₂ is separated and captured from the
95 effluent gas produced during fossil fuel combustion [4]. Oxy-fuel combustion is the process
96 of burning fuel with pure O₂ instead of air as the primary oxidant [4]. The nitrogen-free and
97 oxygen-rich environment results in a more concentrated CO₂ stream in the final flue gas,
98 leading to easier purification [6].

99 Post-combustion CO₂ capture technologies have gained more interest because of their
100 low technological risk and better compatibility with current gas emission control systems
101 [17]. Specifically, solvent absorption, adsorption with solid sorbents, membrane separation,

102 and cryogenic separation are commonly used for post-combustion CO₂ capture [8].
103 Adsorption is considered the best technique because of its low energy consumption, the
104 ability to use this technology at a wide range of temperatures and pressures, and the ease of
105 adsorbent regeneration, without producing any unfavorable byproducts [9]. Various
106 adsorbents such as zeolite, mesoporous carbon, engineered carbon nanomaterials, and
107 activated carbon have been studied for use as CO₂ adsorbents over past few years [10]. Even
108 though these materials show good adsorption performance for capturing CO₂, their use on a
109 large scale is associated with some drawbacks such as adsorption competition and high cost
110 [11].

111 Biochar is a porous carbonaceous material produced through the thermochemical
112 conversion of organic material in oxygen-depleted conditions which is also known as
113 pyrolysis [12] and at moderate temperatures usually below 700 °C [13],[14]. Recently,
114 biochar has been used for various environmental applications including soil quality
115 improvement [15], removal of emerging contaminants in soil [16],[17] and water [18],
116 mitigation of greenhouse gas emissions [19], and energy production [20],[21]. The potential
117 for using biochar for various environmental applications varies with the properties of the
118 biochar, which are affected by the feedstock type and production conditions [22],[23]. As
119 biochar can be produced using abundant biomass and waste, such as crop residues [24],[25],
120 wood waste [24],[26], animal manure, and food waste [27], municipal solid waste [28],
121 sewage sludge [29] it is regarded as an environmentally friendly material for capturing CO₂
122 [30],[31]. In addition, use of waste-derived biochar for CO₂ capture will facilitate sustainable
123 waste management. Activated carbon is being widely used as an adsorbent for removal of
124 various environmental contaminants. Despite of its excellent adsorption capacity, high cost
125 and difficulties in regeneration limit the use of activated carbon as an effective adsorbent
126 [32]. The break-even price of biochar is approximately one sixth of that of activated carbon

127 [13]. In general activated carbon is produced under higher temperature (800-1000 °C) [12]
128 and an additional activation process is crucial in activated carbon production inquiring more-
129 energy consumption and a higher cost compared to biochar which is usually produced at a
130 lower temperature (<700 °C) and activation is unnecessary for biochar production [13],[33].
131 Moreover, the average energy demand for activated carbon production (97 MJ/kg) is
132 significantly higher than that of biochar (6.1 MJ/kg) [34]. Biochar production from waste
133 biomass can benefit both carbon abatement and sustainable management. Carbon dioxide in
134 the atmosphere is first removed by green plants through photosynthesis part of which will
135 then bound to the final carbonaceous structure of biochar without liberating [14],[19]. The
136 economic feasibility of biochar production is highly contingent up the cost of feedstock, and
137 waste biomass serves as economic feedstocks for biochar production in view of its relatively
138 low cost or even income generating potential in the form of tipping fees [35]. Hence, waste
139 based biochar production is considered as a potential sustainable process

140 At present, there is much interest in the scientific community in enhancing the
141 adsorption capacity of biochar by modifying its structure and surface properties [36]. The
142 product that is obtained by modification of pristine biochar (unmodified normal biochar) through
143 physical, chemical and biological methods to improve its physical, chemical and biological properties
144 is known as engineered biochar [37]. Because of the high surface area and porous structure of
145 engineered biochar, it can be used as a potent CO₂ adsorbent [30]. Thus, this review aims to
146 evaluate and summarize the potential of using pristine and engineered biochar as a CO₂
147 capturing medium. It also discusses the factors influencing the CO₂ adsorption capacity of
148 biochar as well as relevant issues related to the synthesis of biochar-based CO₂ adsorbents.

149 150 **2. Biochar as a potential CO₂ adsorbent**

151 Biochar is an eco-friendly adsorbent that is produced from natural biomass or
152 agricultural waste. Biochar is nearly ten times cheaper than other CO₂ adsorbents because of
153 the wide availability of biomass [38]. Raw biochar exhibits a low adsorption capacity towards
154 CO₂, but modified biochar has shown enhanced CO₂ adsorption in many studies. Several
155 modification methods have been tested and applied with varying degrees of success (Section
156 4).

157 Many studies have suggested that the introduction of basic nitrogen functional
158 groups would enhance the basic sites on biochar and increase the uptake of acidic CO₂ [39].
159 Considering that the amine modification of biochar results in a superior surface chemistry for
160 the uptake of CO₂, chicken manure was converted to biochar by pyrolysis at 450 °C for 1 h,
161 followed by chemical treatment with HNO₃ and ammonia gas for 1 h at 450 °C [39]. The
162 modified biochar was further treated with sodium α -L-gulopyranuronate to produce compact
163 beads for easy sorting after the process. The biochar beads had a specific surface area of
164 328.6 m²/g with high adsorption capacity. To increase the nitrogen content and the micro-
165 porosity of the adsorbent, Zhang *et al.* [40] investigated the high-temperature ammonia
166 treatment of biochar with CO₂ activation. The micropore volume of the biochar and CO₂
167 adsorption capacity showed a direct correlation in their study. Studies investigating the CO₂
168 and NH₃ activation of biochar for CO₂ adsorption have been conducted with cotton stalk
169 biochar by Xiong *et al.* [41]. The maximum specific surface area of the CO₂-modified char
170 (610.04 m²/g) was higher than that of the NH₃-modified char (348.56 m²/g) at 800 °C. The
171 CO₂ uptake capacity of CO₂-modified biochar was 100 mg/g (at 20 °C).

172 The performance of virgin and amine-modified biochar (coconut shell) has also been
173 assessed [42]. It was reported by the authors that amine-modified biochar pyrolyzed at
174 800 °C presented the highest adsorption of CO₂ that was reported to be 35.57 mg/g at 30 °C.
175 The authors also reported that the amine treatment of biochar was important because it

176 increased the number of nitrogen-containing functional groups and basicity, which increased
177 the overall CO₂ adsorption. In addition, the potential of untreated and amine-treated sawdust
178 biochar was also evaluated for CO₂ adsorption [43]. In contrast to other studies, this study
179 showed lower CO₂ adsorption in the modified biochar than the unmodified biochar. The
180 reason for the lower CO₂ uptake by the modified biochar was attributed to the incorporation
181 of nitrogen functional groups on the carbon surface, which resulted in the pore obstruction of
182 the amine film and inhibited the CO₂ uptake. Three different ammoxidation methods were
183 studied by Liu *et al.* [44] to prepare biochar from coffee grounds: (i) dispersion of carbonized
184 carbon from the coffee grounds in alcohol containing 3-aminopropyltrimethoxysilane
185 (APTES) followed by refluxing and washing, (ii) dispersion of carbonized carbon from
186 coffee grounds in HCl and treatment by the polycondensation of C₆H₅NH₂ by K₂Cr₂O₇ in an
187 ice bath for 6 h followed by washing and drying, and (iii) dissolution of carbonized carbon
188 from coffee grounds in H₂O via sonication, addition of melamine into the solution,
189 hydrothermal treatment at 160 °C for 24 h, and, finally, drying at 60 °C. The prepared
190 products were chemically activated with KOH and heated to 400 °C for 1 h, followed by
191 ramping to 600 °C for a further hour. The adsorption capacity was 89.78–117.51 mg/g. The
192 adsorbent prepared by method (iii) and after the KOH treatment exhibited the maximum CO₂
193 removal (117.51 mg/g) compared to the other adsorbents prepared in this study. A possible
194 reason for this observation is the well-developed microporous structure, high nitrogen
195 doping, and creation of active sites for adsorption in this particular adsorbent (i.e., that
196 prepared via method (iii)).

197 A two-stage biochar activation process for removal of CO₂ has been reported
198 recently based on ultrasound treatment and amine functionalization [38]. In this process,
199 pinewood-derived biochar was first physically activated by 30-s sonication at ambient
200 temperature. The authors stressed the need for ultrasound treatment because it resulted in the

1
2
3
4
5
6
7
8
9
10
11
12
13
14
15
16
17
18
19
20
21
22
23
24
25
26
27
28
29
30
31
32
33
34
35
201 exfoliation and breaking up of the irregular graphitic layers of the biochar, which resulted in
202 the formation of new micropores. As a result, the porosity and permeability of the biochar
203 were increased, resulting in a higher CO₂ uptake. In the second step, tetraethylenepentamine
204 (TEPA) was used to functionalize the biochar. The adsorption capacity of the biochar
205 modified with ultrasonic treatment followed by TEPA (2.79 mmol/g) was more than nine
206 times more efficient than the untreated biochar [38].

207 Although the pyrolysis method has been widely studied, some researchers have
208 raised concerns about this method because of the high costs associated with the equipment
209 and energy usage. To search for a cheaper, quicker, and more efficient pyrolysis method,
210 Huang *et al.* [45] considered using microwave pyrolysis to produce biochar. In their study,
211 biochar was prepared from rice straw by microwave pyrolysis (200 W and 300 °C). The CO₂
212 removal capacity was found to be up to 80 mg/g at 20 °C, and a correlation between the CO₂
213 removal and the specific surface area was reported. Microwave pyrolysis was suggested to be
214 a better approach than conventional pyrolysis because of its advantages, energy recovery, and
215 zero carbon emissions.

216 Xu *et al.* [46] considered that the presence of alkali or alkali earth metals in the
217 biochar was important for the sorption of the acidic CO₂ molecule. Biochars were developed
218 from sewage sludge, wheat straw, and pig manure by, pyrolyzed at 500 °C for 4 h and tested
219 for carbon dioxide adsorption. The removal of CO₂ was suggested to be induced by
220 mineralogical reactions because minerals such as magnesium, calcium, iron, and potassium
221 were present in the biochar. It was reported that Fe(OH)₂CO₃ was formed in sewage sludge
222 biochar by the transformation of FeOOH after the sorption of CO₂, whereas K₂Ca(CO₃)₂ and
223 CaMg(CO₃)₂ were the transformation products in pig manure after CO₂ sorption. The reaction
224 between adsorbed CO₂ and calcium carbonate (CaCO₃) resulted in the formation of
225 Ca(HCO₃)₂ in the case of wheat straw biochar. The prepared biochars show considerably high

226 sorption efficacy for CO₂ removal (18.2–34.4 mg/g at 25 °C). Guo *et al.* [5] used zinc
227 chloride as a catalyst to synthesize biochar from waste roasted peanut shell by pyrolysis. The
228 developed biochar had a large surface area (1087 m²/g). The capacity for CO₂ adsorption was
229 found to increase with increasing gas pressure and decreasing temperature. The CO₂ removal
230 capacity of the prepared biochar at 100 kPa was reported to be 3.8 mmol/g at 273 K and
231 2.2 mmol/g at 298 K.

232 Single-step pyrolysis at various temperatures (500, 700, and 900 °C) was used to
233 prepare biochars from walnut shells under a N₂ atmosphere [47]. The biochar prepared at
234 900 °C had a high specific surface area (397.015 m²/g) and high microporosity (0.159 cm³/g).
235 Metal impregnation was done followed by heat treatment with nitrogen. For metal
236 impregnation, metal nitrate salts of sodium, magnesium, calcium, nickel, iron, and aluminum
237 were selected. It was reported that the addition of basic sites (induced by metal impregnation)
238 on the surface of biochar improved the removal of CO₂. The performance of the metal-
239 impregnated biochar followed the order: magnesium > aluminum > iron > nickel >
240 calcium > raw biochar > sodium. The magnesium-loaded biochar exhibited a higher CO₂
241 uptake (82.0 mg/g) than the virgin biochar (72.6 mg/g) at 25 °C and 1 atm. The improved
242 performance of the modified biochar was explained as resulting from combined physical and
243 chemical effects.

244 Sugarcane bagasse and hickory wood were pyrolyzed at three different temperatures
245 (300, 450, and 600 °C) under a N₂ atmosphere for the production of biochar for CO₂ removal
246 [48]. The CO₂ adsorption capacities of the prepared biochars were found to be in the range of
247 34.48–73.55 mg/g at 25 °C and 11.15–43.67 mg/g at 75 °C. The larger surface area of the
248 biochars and the presence of nitrogen-containing groups on the biochar surface was suggested
249 to contribute toward the CO₂ capture. The biochar prepared from bagasse samples possessed
250 a larger number of nitrogen-containing functional groups than the hickory samples and,

1 251 consequently, exhibited better CO₂ removal. Creamer *et al.* [49] hypothesized that basic
2 252 metal oxyhydroxides can easily interact with acidic CO₂ when the polar surfaces are in
3
4 253 contact. To test this hypothesis, the authors prepared metal-oxyhydroxide–biochar
5
6 254 composites and assessed them for CO₂ adsorption. Raw cottonwood was used to prepare the
7
8 255 biochar, and the biochar was treated with the chloride salts of three metals (Al, Fe, and Mg).
9
10 256 The mixture (cottonwood in metal salt) was pyrolyzed at 600 °C under a nitrogen atmosphere
11
12 257 for 3 h. It was found that, in comparison with the raw biochar (58 mg/g), the metal-modified
13
14 258 biochars displayed higher CO₂ adsorption, i.e., 27–63 mg/g for Mg biochar, 54–67 mg/g for
15
16 259 Fe biochar, and 63–71 mg/g for Al biochar.
17
18
19
20
21

22 260 Single-step activation of biomass (almond shells and olive stones) in air at 400–500
23
24 261 °C and at a low oxygen content (3–5%) in the activating gas at high temperatures (500–
25
26 262 650 °C) has also been reported [50]. Samples that were activated at 650 °C showed the
27
28 263 highest CO₂ adsorption capacity. The almond-shell-based chars exhibited a CO₂ removal of
29
30 264 up to 2.1 mmol/g at 25 °C and 0.7 mmol/g at 100 °C. These results were discussed by authors
31
32 265 based on micropore volume and pore diameters. Four types of feedstocks, namely soybean
33
34 266 stover, perilla leaf, Japanese oak, and Korean oak, were used to prepare different types of
35
36 267 biochars [51]. The powdered biomass was pyrolyzed at 700 °C, and the Korean oak and
37
38 268 Japanese oak biochars were produced at 400 and 500 °C, respectively. The efficiency of the
39
40 269 prepared biochars for CO₂ adsorption was found to decrease in the order Perilla leaf (2.312
41
42 270 mmol/g) > Korean oak (0.597 mmol/g) > Japanese oak (0.379 mmol/g) > soybean stover
43
44 271 (0.707 mmol/g), and this was related to the nitrogen contents of these biochars. In addition to
45
46 272 the above-mentioned studies, other researchers have also investigated biochars for CO₂
47
48 273 adsorption [52],[53].
49
50
51
52
53
54
55
56
57 274
58
59
60
61
62
63
64
65

1
2
3
4
5
6
7
8
9
10
11
12
13
14
15
16
17
18
19
20
21
22
23
24
25
26
27
28
29
30
31
32
33
34
35
36
37
38
39
40
41
42
43
44
45
46
47
48
49
50
51
52
53
54
55
56
57
58
59
60
61
62
63
64
65

275 3. Biochar properties influencing CO₂ adsorption

276 The CO₂ adsorption capacity of biochar, which is the amount of CO₂ adsorbed per unit
277 weight of biochar, mainly depends on the physicochemical properties of the biochar, such as
278 the surface area, pore size, pore volume, basicity of biochar surface, presence of surface
279 functional groups, presence of alkali and alkali earth metals, hydrophobicity, polarity, and
280 aromaticity [54]. These physical and chemical properties of biochar are closely related to the
281 type of feedstock used and the thermochemical conditions of biochar production [55],[56].
282 Table 1 summarizes the effects of feedstock type and pyrolysis conditions on the properties
283 of the biochar.

284 285 3.1 Physical properties of biochar

286 Carbon dioxide adsorption occurs through van der Waals forces between gas molecules
287 and the solid phase (biochar), which is associated with the specific surface area, pore size,
288 and pore volume of the biochar [57].

290 **Table 1.** Effect of feedstock and pyrolysis conditions on the biochar properties

Type of feedstock	Pyrolysis conditions	C (%)	H (%)	O (%)	N (%)	Surface area (BET) (m ² /g)	Pore diameter (nm)	Pore volume (cm ³ /g)	Reference
Vegetable waste	200 °C for 2 h	52.89	6.9	36.02	4.2	0.36	2.59	43.24	[58]
Vegetable waste	500 °C for 2 h	83.85	2.7	9.73	3.71	50.26	3.22	54.61	[58]
Pine cone	200 °C for 2 h	69.74	2.13	27.09	1.03	0.47	2.38	45.13	[58]
Pine cone	500 °C for 2 h	74.64	2.62	20.94	1.81	192.97	10.2	2.44	[58]
Pitch pine wood chips	300 °C fast pyrolysis	63.9	5.4	30.4	0.3	2.9	N/A	N/A	[59]
Pitch pine wood chips	400 °C fast pyrolysis	70.7	3.4	25.5	0.4	4.8	N/A	N/A	[59]
Pitch pine wood chips	500 °C fast pyrolysis	90.5	2.5	6.7	0.3	175.4	N/A	N/A	[59]
Rubber wood sawdust	300 °C for 1-h	N/A	N/A	N/A	N/A	1.8	7.4	0.0032	[60]
Rubber wood sawdust	400 °C for 1 h	N/A	N/A	N/A	N/A	1.4	9.6	0.0034	[60]
Rubber wood sawdust	500 °C for 1 h	N/A	N/A	N/A	N/A	2.2	11	0.0061	[60]
Rubber wood sawdust	600 °C for 1 h	N/A	N/A	N/A	N/A	2.7	11.8	0.008	[60]
Rubber wood sawdust	700 °C for 1 h	N/A	N/A	N/A	N/A	2.3	15.8	0.0089	[60]
Rubber wood sawdust	300 °C for 3 h	N/A	N/A	N/A	N/A	1.9	7.0	0.0034	[60]
Rubber wood sawdust	400 °C for 3 h	N/A	N/A	N/A	N/A	2.1	12.4	0.0066	[60]
Rubber wood sawdust	500 °C for 3 h	N/A	N/A	N/A	N/A	2	12.7	0.0064	[60]
Rubber wood sawdust	600 °C for 3 h	N/A	N/A	N/A	N/A	1.9	13	0.0063	[60]
Rubber wood sawdust	700 °C for 3h	N/A	N/A	N/A	N/A	5.5	7.0	0.0097	[60]
Wheat straw	400 °C for 1.5 h	57.8	3.2	21.6	1.5	10	4.6	0.012	[61]
Wheat straw	500 °C for 1.5 h	70.3	2.9	17.7	1.4	111	3.3	0.09	[61]
Wheat straw	600 °C for 1.5 h	73.4	2.1	14.9	1.4	177	2.5	0.11	[61]
Wheat straw	700 °C for 1.5 h	73.9	1.3	14.6	1.2	107	2.2	0.058	[61]
Corn straw	400 °C for 1.5 h	56.1	4.3	22	2.4	4	8.1	0.008	[61]
Corn straw	500 °C for 1.5 h	58	2.7	21.5	2.3	6	2.1	0.012	[61]
Corn straw	600 °C for 1.5 h	58.6	2	18.7	2	7	6.3	0.012	[61]
Corn straw	700 °C for 1.5 h	59.5	1.5	16.6	1.6	3	8.2	0.006	[61]
Peanut shell	400 °C for 1.5 h	58.4	3.5	21	1.8	5	5.2	0.007	[61]
Peanut shell	500 °C for 1.5 h	64.5	2.8	18.5	1.7	28	3.2	0.022	[61]
Peanut shell	600 °C for 1.5 h	71.9	2	15	1.6	195	2.4	0.11	[61]

1
2
3
4
5
6
7
8
9
10
11
12
13
14
15
16
17
18
19
20
21
22
23
24
25
26
27
28
29
30
31
32
33
34
35
36
37
38
39
40
41
42
43
44
45
46
47
48
49

Type of feedstock	Pyrolysis conditions	C (%)	H (%)	O (%)	N (%)	Surface area (BET) (m ² /g)	Pore diameter (nm)	Pore volume (cm ³ /g)	Reference
Peanut shell	700 °C for 1.5 h	74.4	1.4	14.2	1.4	49	2.7	0.033	[61]
Wood	850 °C for 3 h	84.5	1.0	N/A	0.5	172	N/A	0.121	[62]
Wood chip (70%) + chicken manure (30%)	850 °C for 3 h	70.7	2.1	N/A	0.7	342	N/A	0.224	[62]
Yak manure	300 °C for 3 h	41.6	1.9	27.4	3.2	3.6	11.3	N/A	[63]
Yak manure	500 °C for 3 h	41.3	1.7	24.4	3.0	17.3	7.5	4.4	[63]
Yak manure	700 °C for 3 h	41.2	1.4	20.7	2.7	82.9	3.6	52.8	[63]
Sewage sludge	500 °C for 4 h	29.1	1.56	N/A	3.34	10.12	N/A	0.022	[46]
Pig manure	500 °C for 4 h	47.7	1.91	N/A	2.49	31.57	N/A	0.044	[46]
wheat straw	500 °C for 4 h	60.5	2.31	N/A	0.97	20.2	N/A	0.041	[46]
Rice straw	300 °C for 1.5 h	N/A	N/A	N/A	N/A	3.35	151.3	0.127	[64]
Rice straw	500 °C for 1.5 h	N/A	N/A	N/A	N/A	7.47	108.1	0.0202	[64]
Rice straw	700 °C for 1.5 h	N/A	N/A	N/A	N/A	32.9	59.2	0.0486	[64]
Pig manure	300 °C for 1.5 h	N/A	N/A	N/A	N/A	3.32	229.9	0.0191	[64]
Pig manure	500 °C for 1.5 h	N/A	N/A	N/A	N/A	6.3	184.5	0.0291	[64]
Pig manure	700 °C for 1.5 h	N/A	N/A	N/A	N/A	20.5	88.4	0.0454	[64]
Rice straw (hydrochar)	300 °C for 1.5 h	N/A	N/A	N/A	N/A	2.57	314.1	0.0202	[64]
Rice straw (hydrochar)	700 °C for 1.5 h	N/A	N/A	N/A	N/A	2.94	174.3	0.0128	[64]
Pig manure (hydrochar)	300 °C for 1.5 h	N/A	N/A	N/A	N/A	15.5	233.5	0.0907	[64]

1
2
3
4
5
6
7
8
9
10
11
12
13
14
15
16
17
18
19
20
21
22
23
24
25
26
27
28
29
30
31
32
33
34
35
36
37
38
39
40
41
42
43
44
45
46
47
48
49

291

Type of feedstock	Pyrolysis conditions	C (%)	H (%)	O (%)	N (%)	Surface area (BET) (m ² /g)	Pore diameter (nm)	Pore volume (cm ³ /g)	Reference
Pig manure (hydrochar)	500 °C for 1.5 h	N/A	N/A	N/A	N/A	15.6	310.6	0.1212	[64]
Pig manure (hydrochar)	700 °C for 1.5 h	N/A	N/A	N/A	N/A	10.7	272.7	0.0728	[64]

3.1.1 Specific surface area

The specific surface area of biochar can be defined as the ratio between the total surface area and the total mass of the biochar [65]. Several studies have assessed the effects of the specific surface area of biochar on its capacity of CO₂ adsorption [46]. A positive relationship ($R^2 = 0.6475$, $n = 16$) can be seen between the specific surface area and the CO₂ adsorption capacity of biochar (Fig. 1a). A larger surface area provides more active sites for CO₂ adsorption through physical adsorption; thus, a higher biochar surface area leads to a correspondingly larger adsorption capacity [10].

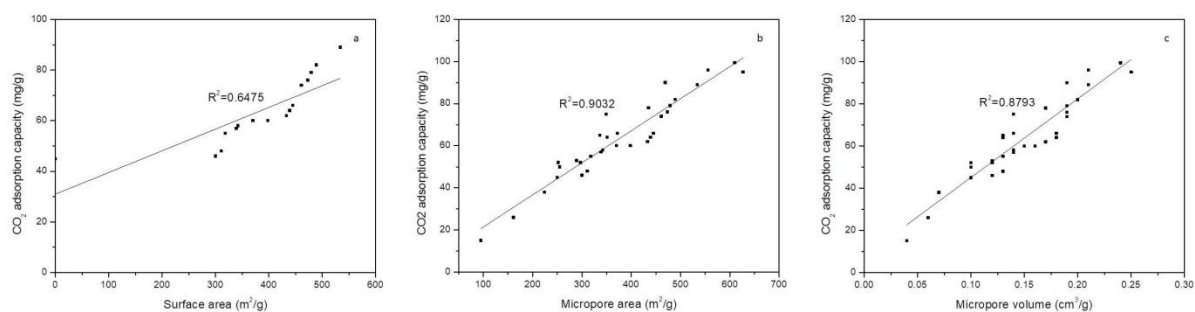


Fig. 1. Relationship between the (a) specific surface area, (b) micropore area, (c) micropore volume, and CO₂ adsorption capacity of biochar (Data was obtained from [66], [67]).

The specific surface area of biochar is strongly related to the carbon content of the material, which may vary depending on the feedstock [65],[68]. However, high mineral content can reduce the specific surface area by blocking the pores on the biochar surface [69]. The Brunauer–Emmett–Teller (BET) specific surface area of corn-straw-derived biochar is lower than that of the biochars derived from peanut shell and wheat straw, suggesting that this difference can be attributed to the different lignin, cellulose, and hemicellulose contents of the feedstock, which may also contribute to different decomposition rates (Fig. 2a) [61]. Biochar produced from plant materials such as corn stove, oak wood, and pine needles showed significantly higher surface areas than that of the biochar produced from animal litter such as swine manure and biosolid waste (Table 1) [18],[55]. Nevertheless, a study conducted

1 313 with 100% wood-derived biochar and that prepared from 70% wood + 30% chicken manure
2 314 showed BET surface areas of 172 and 342 m²/g, respectively, which could be attributed to the
3
4 315 feedstock (Table 1) [62]. In general, wood chips are larger than chicken manure granules and
5
6
7 316 wood chips have a higher fixed carbon content than chicken manure (Fig. 2b), which may
8
9 317 cause a lower burn off rate, thus contributing to a lower surface area and porosity [62].
10

11
12 318 The surface area of the biochar increases with increasing pyrolysis temperature and
13
14 319 residence time, possibly because of the release of volatile matter, which increases the pore
15
16 320 volume [18]. For instance, increasing temperature from 200 °C to 500 °C in biochar produced
17
18
19 321 with vegetable waste and pine cone enhanced the surface area from 0.36 to 50.26 and 0.47 to
20
21 322 192.97 m²/g respectively (Table 1) [58]. The mobile matter content was reduced from 56.44
22
23
24 323 to 12.43 and 62.35 to 10.01 % respectively when the temperature was increased from 200 °C
25
26 324 to 500 °C in biochar produced with vegetable waste and pine cone (Fig. 2c) [58]. This
27
28
29 325 suggested that release of mobile matter would open up the pores in biochar matrix enhancing
30
31 326 surface area. In addition, increase in the temperature from 300 to 500 °C was found to
32
33
34 327 increase the specific surface area of pitch pine wood biochar from 2.9 to 175.4 m²/g [59].
35
36 328 Moreover, a study conducted with wheat straw, corn straw, and peanut shell biochars
37
38
39 329 revealed that the surface area of the biochar increased substantially from 300 to 600 °C,
40
41 330 whereas a reduction was observed at 700 °C irrespective of the feedstock, suggesting the loss
42
43
44 331 of H and O-containing functional groups, whereas aliphatic alkyl CH₂, aromatic CO, ester
45
46 332 C₅O, and OH groups serve to increase the surface area at 600 °C [61],[70]. A significant
47
48
49 333 increase in the BET surface area of rubber wood sawdust biochar was observed at 700 °C
50
51 334 after a residence time of 3 h [60]. It was suggested that the partially carbonized reactants may
52
53
54 335 lower the surface area at lower temperatures, and the high temperature (700 °C) led to the
55
56 336 release of a higher amount of volatile organic compounds, thus creating more pores [60].
57
58
59
60
61
62
63
64
65

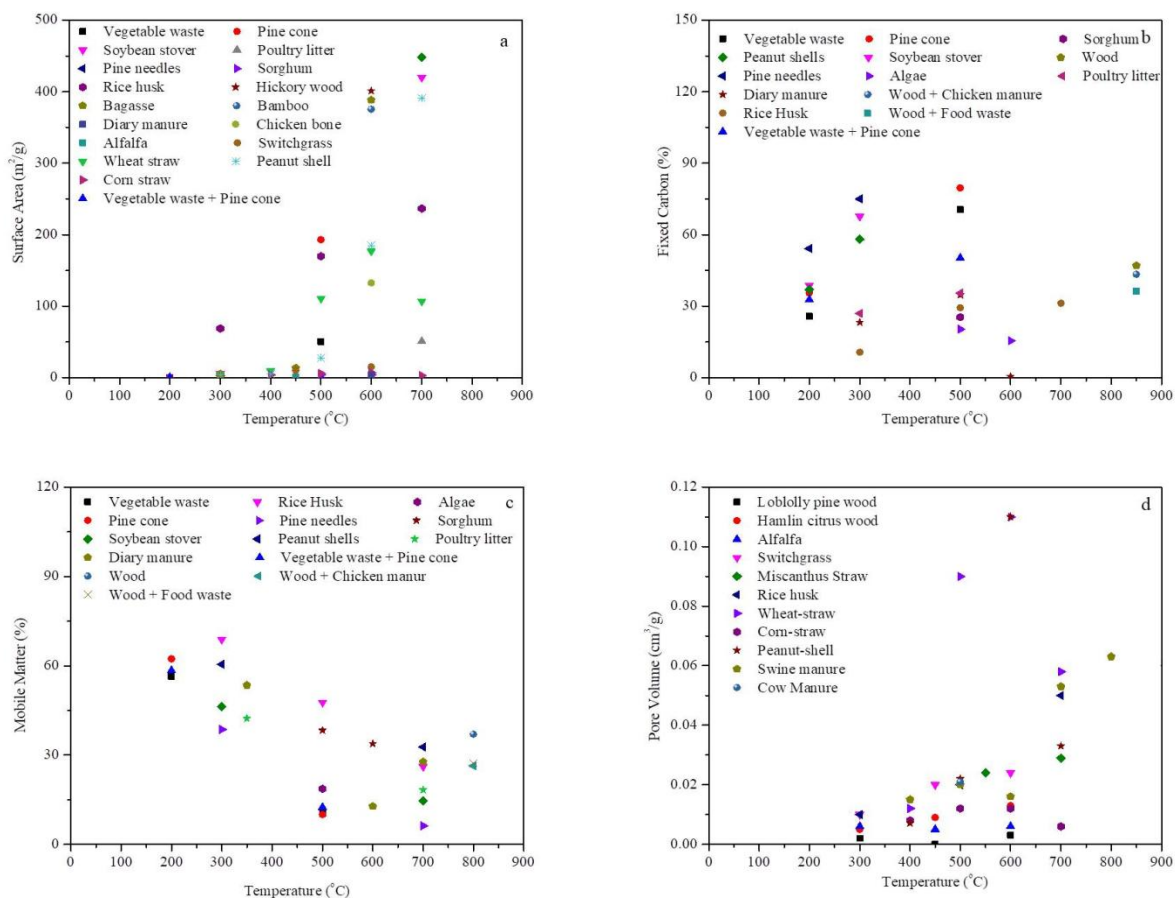


Fig. 2. Variation of (a) surface area, (b) fixed carbon content, (c) mobile matter content and (d) pore volume of biochar produced from different feedstock types under different pyrolysis temperatures (Data was obtained from [27], [58], [61], [71], [72], [73], [74], [75], [76], [77], [78])

3.1.2 Total pore volume and pore size

The pore volume and pore size also play a vital role in CO₂ adsorption. The release of volatile organic matter from the polymeric backbone of the feedstock causes the formation of porous structures in the biochar, and a larger total pore volume provides more active sites for interaction between CO₂ and the biochar [65],[79]. Per the pore size classification of the International Union of Pure and Applied Chemistry, pores with a diameter greater than 50 nm are categorized as macropores, those with a diameter between 2 and 50 nm are mesopores,

1 and those with a diameter of less than 2 nm are micropores [65]. Generally, the CO₂ capture
2 capacity of porous carbon strongly depends on the presence of micropores with a diameter of
3 less than 1 nm[80],[81]. Nevertheless, studies have revealed that pores with a diameter of 0.5
4 nm or less contribute significantly to CO₂ adsorption at low partial pressures, whereas pores
5 with a diameter smaller than 0.8 nm make a higher contribution to CO₂ uptake at 1 bar [82].
6
7 The CO₂ adsorption capacity has a stronger correlation with the micropore surface area ($R^2 =$
8 0.9032 , $n= 32$, Fig. 1b) than the BET surface area ($R^2 = 0.6475$, $n=16$, Fig. 1a), suggesting
9 that the micropore structure of the biochar significantly affects the CO₂ adsorption capacity
10 [67]
11
12
13
14
15
16
17
18
19
20
21

22 A study conducted to assess the effect of the pyrolysis temperature on the pore volume
23 showed that there is an increase in the micropore volume and the total pore volume of the
24 biochar as the temperature increases from 400 to 500 °C and a reverse trend is observed when
25 the temperature is increased above 500 °C (Table 1, Fig 2d) [83]. When the temperature is
26 higher than 500 °C, the coalescence of neighboring pores can widen the pores while reducing
27 the pore volume [83]. Furthermore, even during modification of biochar using different
28 compounds, the micropore volume and surface area of the micropores increase with
29 increasing modification temperature but begin to decrease from 800 °C because of the
30 coalescence of micropores and increase in mesopores and macropores [41],[67].
31
32
33
34
35
36
37
38
39
40
41
42

43 Anglin et al [83] also observed a reduction in pore volume with the increase of heating
44 rate from 10 to 50 °C/min. When the heating rate of the process is low, pyrolysis
45 products/volatile organic matter has enough time to diffuse from the biochar particles.
46 Nevertheless, with the increase of heating rate, the time for discharging volatile organic
47 matter reduces resulting in the accumulation of volatiles within and between particles
48 blocking the pore entrance [83].
49
50
51
52
53
54
55
56
57
58
59
60
61
62
63
64
65

375 3.2 Chemical properties of biochar

1
2 376 The adsorption of CO₂ onto the biochar surface is also affected by the chemical
3
4
5 377 properties of the biochar such as alkalinity, mineral composition, presence of surface
6
7 378 functional groups, hydrophobicity, and non-polarity [46],[84]. The CO₂ adsorption capacity
8
9 379 of biochar can be enhanced by increasing the alkalinity of the biochar surface [47].
10

11 380

14 381 3.2.1 Basic functional groups

16
17 382 The presence of basic surface functional groups plays an important role in the CO₂
18
19 383 adsorption of biochar because of their contribution to surface basicity, which enhances the
20
21 384 affinity of the biochar for CO₂ [85]. Nitrogen-containing functional groups (e.g., amide,
22
23 385 imide, pyridinic, pyrrolic, and lactam groups) are the contributors to the surface basicity of
24
25 386 biochar. They can be introduced to the biochar surface through reaction with different N-
26
27 387 containing reagents such as ammonia, amines, and nitric acid or by the activation of biochar
28
29 388 with nitrogen-containing precursors (a precursor is a compound that participates in a
30
31 389 chemical reaction while producing another compound), such as melamine or polyacrylonitrile
32
33 390 [5],[86]. The Fourier transform infrared spectroscopy (FTIR) spectrum of ammonia-modified
34
35 391 biochar shows C = N (1745 - 1586 cm⁻¹) and C-N (1056 cm⁻¹) stretches corresponding to N-
36
37 392 containing functional groups [57]. Moreover, the authors observed the highest CO₂
38
39 393 adsorption capacity (39.37 mg/g) in the ammonia-modified biochar [57]. In addition, some
40
41 394 oxygen-containing functional groups such as ketones, pyrones, and chromenes also contribute
42
43 395 to the surface basicity. Xing *et al.* [87] suggested that the basicity of N-containing functional
44
45 396 groups is very weak compared to that of organic amines, but this has rarely been studied.
46
47 397 Unlike the acid–base interaction between CO₂ and the biochar surface, there is evidence that
48
49 398 the presence of oxygen-containing acidic functional groups such as hydroxyl groups,
50
51 399 carboxyl groups, and carbonyl groups also increase CO₂ adsorption on carbonaceous surfaces
52
53
54
55
56
57
58
59
60
61
62
63
64
65

1 400 by facilitating hydrogen bonding between the CO₂ molecules and the carbon surface
2 401 [87],[88].
3

4 402

7 403 3.2.2 Alkaline and alkaline earth metals

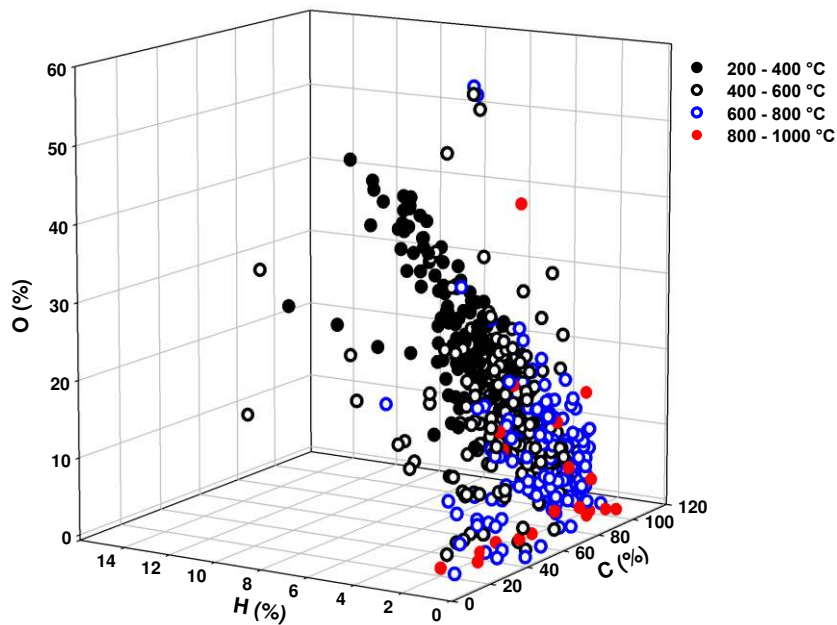
9 404 The presence of alkali metals and alkaline earth metals (e.g., Na, K, Ca, Mg, and Li)
10
11 405 can enhance the formation of basic sites with a strong affinity for CO₂, which has an acidic
12
13 406 nature [46]. Thus, the presence of alkaline metals and alkaline earth metals may enhance the
14
15 407 CO₂ adsorption capacity of biochar. For instance, when biochar is loaded with Mg(NO₃)₂,
16
17 408 MgO is formed when the temperature is above 400 °C which facilitate CO₂ adsorption
18
19 409 through the interaction between CO₂ and O₂ [47]. However, the reaction between O₂⁻ and
20
21 410 CO₂ forms a monolayer of magnesium carbonate (MgCO₃) on the surface which limits the
22
23 411 further reaction between MgO and CO₂ [89]. Additionally, decrease in the specific surface
24
25 412 area and pore volume have been observed with the incorporation of metal ions due to
26
27 413 localized deposition of metals on the biochar surface and blockage of micropore entrance by
28
29 414 magnesium oxide [47].
30
31
32
33
34
35

36 415

38 416 3.2.3 Hydrophobicity, polarity, and aromaticity

40
41 417 Studies have revealed that the CO₂ adsorption capacity of carbonaceous materials
42
43 418 may be reduced under humid environments because of the high affinity for H₂O of most
44
45 419 porous materials [90],[91]. Thus, biochar with hydrophobic and non-polar characteristics may
46
47 420 facilitate the CO₂ adsorption capacity by hindering the competition of H₂O molecules. Low
48
49 421 H/C and O/C ratios (< 0.2), suggest a high degree of aromaticity and fixed carbon, which are
50
51 422 chemically stable [65]. Very low O/C ratios have been found in white oak biochar (O/C =
52
53 423 0.051), and this is associated with high hydrophobicity, low polarity, and enhanced CO₂
54
55 424 capturing capacity of biochar [92]. Increasing pyrolysis temperature can separate H and O
56
57
58
59
60
61
62
63
64
65

425 due to the fracture of chemical bonds. The molar ratio of O/C and H/C decreases as the
426 increase of pyrolysis temperature (Table 1), possibly due to loss of volatile organic
427 compounds and increase in dehydrogenation and deoxygenation reactions resulting formation
428 of aromatic structures and reduce the polarity of biochar while increasing the hydrophobicity
429 (Fig. 3) [31],[60],[77],[93],.



431
432 Fig. 3. Variation of carbon (C), hydrogen (H), and oxygen (O) (percentages) in biochar with
433 the pyrolysis temperature. (Adopted from Igalavithana et al., [94])

435 4. Modified biochar for CO₂ adsorption

436 Biochar has excellent inherent characteristics for capturing CO₂ because of its polar and
437 hydrophilic nature with a highly porous structure and high specific surface area [18],[48],[95]
438 . At present, scientists focus on the production of engineered/designer biochar through
439 modification with novel structures to yield different surface properties and increase the
440 sorption capacity [11],[96]. The modification of biochar can be achieved through various
441 methods, such as the use of different activation conditions, precursors, and additives

1 442 [97],[98]. The feedstock can be treated either prior to pyrolysis or after pyrolysis to achieve
2 443 the desired changes to the biochar [94]. The modification of biochar can be categorized as
3
4 444 chemical modification, physical modification, impregnation with elements, or grafting [99].
5
6
7 445 Table 2 summarizes the key findings of recent research on the use of modified biochar for
8
9 446 CO₂ adsorption.

14 448 4.1 Alkali-modified biochar

16
17 449 The activation of biochar using KOH or NaOH dissolves ash and compounds like lignin
18
19 450 and cellulose, which increases the O content and surface basicity of the biochar [100],[101].
20
21 451 Two-stage KOH activation of pre-carbonized precursors may create a higher surface area
22
23 452 with more surface hydroxyl groups than that of pristine biochar [102],[103]. Moreover,
24
25 453 during the KOH activation process, different potassium species, including K₂O and K₂CO₃,
26
27 454 are formed and diffuse into the internal structure of the biochar matrix, which increases the
28
29 455 width of the existing pores and generates new pores [104],[105]. Nevertheless, the effect of
30
31 456 alkali treatment on the formation of –OH in biochar depends on the type of feedstock,
32
33 457 charring method, and treatment conditions, such as the activation temperature and ratio
34
35 458 between alkali and C [6],[31]. KOH-activated biochar has been found to yield a higher BET
36
37 459 surface area (1400 m²/g) and higher ultra-micropore and super-micropore volume than those
38
39 460 of CO₂- and steam-activated biochars leading to a significant increase in CO₂ adsorption
40
41 461 capacity in KOH activated biochar than that of steam activated biochar (Table 2) [107].
42
43 462 KOH-activated biochar exhibits higher adsorption capacities than CO₂ and steam-activated
44
45 463 biochar because of its higher surface area and micropore volume, irrespective of the presence
46
47 464 of more oxygen-containing functional groups [5],[107].
48
49
50
51
52
53
54
55
56
57
58
59
60
61
62
63
64
65

1
2
3
4
5
6
7
8
9
10
11
12
13
14
15
16
17
18
19
20
21
22
23
24
25
26
27
28
29
30
31
32
33
34
35
36
37
38
39
40
41
42
43
44
45
46
47
48
49

465 **Table 2.** Effect of biochar modification on its properties and CO₂ adsorption capacity

466

Feedstock	Pyrolysis temperature (°C)	Modification	BET surface area (m ² /g)	Surface area of micropores (m ² /g)	Total pore volume (cm ³ /g)	Micropore volume (cm ³ /g)	Adsorption temperature (°C)	CO ₂ adsorption capacity (mg/g)	Reference
Whitewood	500	Steam activation	840	N/A	0.55	N/A	25	59	[107]
Whitewood	500	CO ₂ activation	820	N/A	0.45	N/A	25	63	[107]
Whitewood	500	KOH activation	1400	N/A	0.62	N/A	25	78	[107]
Soybean straw	500	Raw biochar without activation	0.04	250	N/A	0.1	30	45 (Approx.)	[67]
Soybean straw	500	CO ₂ activation at 500 °C	5.5	300	N/A	0.12	30	46 (Approx.)	[67]
Soybean straw	500	CO ₂ activation at 600 °C	2.6	342	N/A	0.14	30	58 (Approx.)	[67]
Soybean straw	500	CO ₂ activation at 700 °C	22	398	N/A	0.16	30	60 (Approx.)	[67]
Soybean straw	500	CO ₂ activation at 800 °C	346	473	N/A	0.19	30	76 (Approx.)	[67]
Soybean straw	500	CO ₂ activation at 900 °C	397	445	N/A	0.18	30	66 (Approx.)	[67]
Soybean straw	500	Ammonification with NH ₃ at 500 °C	1.5	311	N/A	0.13	30	48 (Approx.)	[67]
Soybean straw	500	Ammonification with NH ₃ at 600 °C	5.8	339	N/A	0.14	30	57 (Approx.)	[67]
Soybean straw	500	Ammonification with NH ₃ at 700 °C	221	433	N/A	0.17	30	62 (Approx.)	[67]
Soybean straw	500	Ammonification with NH ₃ at 800 °C	365	479	N/A	0.19	30	79 (Approx.)	[67]

Feedstock	Pyrolysis temperature (°C)	Modification	BET surface area (m ² /g)	Surface area of micropores (m ² /g)	Total pore volume (cm ³ /g)	Micro pore volume (cm ³ /g)	Adsorption temperature (°C)	CO ₂ adsorption capacity (mg/g)	Reference
Soybean straw	500	Ammonification with NH ₃ at 900 °C	469	461	N/A	0.19	30	74 (Approx.)	[67]
Soybean straw	500	Treatment with CO ₂ -NH ₃ mixture at 500 °C	2	318	N/A	0.13	30	55 (Approx.)	[67]
Soybean straw	500	Treatment with CO ₂ -NH ₃ mixture at 600 °C	1.2	370	N/A	0.15	30	60 (Approx.)	[67]
Soybean straw	500	Treatment with CO ₂ -NH ₃ mixture at 700 °C	41	439	N/A	0.18	30	64 (Approx.)	[67]
Soybean straw	500	Treatment with CO ₂ -NH ₃ mixture at 800 °C	491	534	N/A	0.21	30	89 (Approx.)	[67]
Soybean straw	500	Treatment with CO ₂ -NH ₃ mixture at 900 °C	764	489	N/A	0.2	30	82 (Approx.)	[67]
Cotton stalk	600	Unmodified biochar	N/A	224	N/A	0.07	20	38 (Approx.)	[66]
Cotton stalk	600	Modified with CO ₂ at 500 °C	N/A	289	N/A	0.12	20	53 (Approx.)	[66]
Cotton stalk	600	Modified with CO ₂ at 600 °C	N/A	351	N/A	0.13	20	64 (Approx.)	[66]
Cotton stalk	600	Modified with CO ₂ at 700 °C	N/A	372	N/A	0.14	20	66 (Approx.)	[66]
Cotton stalk	600	Modified with CO ₂ at 800 °C	N/A	610	N/A	0.24	20	99.42 (Approx.)	[66]
Cotton stalk	600	Modified with CO ₂ at 900 °C	N/A	556	N/A	0.21	N/A	96 (Approx.)	[66]
Cotton stalk	600	Modified with NH ₃ 500 °C	N/A	161	N/A	0.06	N/A	26 (Approx.)	[66]

1
2
3
4
5
6
7
8
9
10
11
12
13
14
15
16
17
18
19
20
21
22
23
24
25
26
27
28
29
30
31
32
33
34
35
36
37
38
39
40
41
42
43
44
45
46
47
48
49

Feedstock	Pyrolysis temperature (°C)	Modification	BET surface area (m ² /g)	Surface area of micropores (m ² /g)	Total pore volume (cm ³ /g)	Micro pore volume (cm ³ /g)	Adsorption temperature (°C)	CO ₂ adsorption capacity (mg/g)	Reference
Cotton stalk	600	Modified with NH ₃ 600 °C	N/A	252	N/A	0.1	N/A	52 (Approx.)	[66]
Cotton stalk	600	Modified with NH ₃ 700 °C	N/A	255	N/A	0.1	N/A	50 (Approx.)	[66]
Cotton stalk	600	Modified with NH ₃ 800 °C	N/A	349	N/A	0.14	N/A	75 (Approx.)	[66]
Cotton stalk	600	Modified with NH ₃ 900 °C	N/A	435	N/A	0.17	N/A	78 (Approx.)	[66]
Cotton stalk	600	Modified with CO ₂ and NH ₃ mixture 500 °C	N/A	95	N/A	0.04	N/A	15 (Approx.)	[66]
Cotton stalk	600	Modified with CO ₂ and NH ₃ mixture 600 °C	N/A	297	N/A	0.12	120	52 (Approx.)	[66]
Cotton stalk	600	Modified with CO ₂ and NH ₃ mixture 700 °C	N/A	336	N/A	0.13	N/A	65 (Approx.)	[66]
Cotton stalk	600	Modified with CO ₂ and NH ₃ mixture 800 °C	N/A	627	N/A	0.25	N/A	95 (Approx.)	[66]
Cotton stalk	600	Modified with CO ₂ and NH ₃ mixture 900 °C	N/A	469	N/A	0.19	N/A	90 (Approx.)	[66]
Cotton stalk	600	Unmodified biochar	224.12	N/A	N/A	0.07	20 120	58 14 (Approx.)	[41]
Cotton stalk	600	Modified with NH ₃ at 500 °C	N/A	160.89	N/A	0.06	20 120	46 36 (Approx.)	[41]
Cotton stalk	600	Modified with NH ₃ at 600 °C	N/A	251.91	N/A	0.08	20 120	50 35 (Approx.)	[41]

(Approx.)

Feedstock	Pyrolysis temperature (°C)	Modification	BET surface area (m ² /g)	Surface area of micropores (m ² /g)	Total pore volume (cm ³ /g)	Micro pore volume (cm ³ /g)	Adsorption temperature (°C)	CO ₂ adsorption capacity (mg/g)	Reference
Cotton stalk	600	Modified with NH ₃ at 700 °C	N/A	254.97	N/A	0.14	20 120	60 (Approx.) 28 (Approx.)	[41]
Cotton stalk	600	Modified with NH ₃ at 800 °C	N/A	348.56	N/A	0.17	20 120	72 (Approx.) 13 (Approx.)	[41]
Cotton stalk	600	Modified with NH ₃ at 900 °C	N/A	434.92	N/A	0.19	20 120	78 (Approx.) 10 (Approx.)	[41]
Cotton stalk	600	Modified with CO ₂ at 500 °C	N/A	289.07	N/A	0.12	20 120	64 (Approx.) 10 (Approx.)	[41]
Cotton stalk	600	Modified with CO ₂ at 600 °C	N/A	351.49	N/A	0.13	20 120	54 (Approx.) 12 (Approx.)	[41]
Cotton stalk	600	Modified with CO ₂ at 700 °C	N/A	371.65	N/A	0.14	20 120	72 (Approx.) 13 (Approx.)	[41]
Cotton stalk	800	Modified with CO ₂ at 800 °C	N/A	610.04	N/A	0.24	20 120	96 (Approx.) 20 (Approx.)	[41]
Cotton stalk	600	Modified with CO ₂ at 900 °C	N/A	556.35	N/A	0.21	20 120	80 (Approx.)	[41]

1
2
3
4
5
6
7
8
9
10
11
12
13
14
15
16
17
18
19
20
21
22
23
24
25
26
27
28
29
30
31
32
33
34
35
36
37
38
39
40
41
42
43
44
45
46
47
48
49

16
(Approx.)

Sawdust	450	Unmodified biochar	8.76	N/A	N/A	N/A	30	19.7	[43]
Sawdust	450	Unmodified biochar	8.76	N/A	N/A	N/A	70	13.5	[43]
Sawdust	450	Treatment with monoethanolamine	0.61	N/A	N/A	N/A	30	19.1	[43]
Sawdust	450	Treatment with monoethanolamine	0.61	N/A	N/A	N/A	70	12.1	[43]
Sawdust	450	Treatment with monoethanolamine	0.61	N/A	N/A	N/A	70	12.1	[43]
Sawdust	750	Unmodified biochar	1.36	N/A	N/A	N/A	30	45.2	[43]
Sawdust	750	Unmodified biochar	1.36	N/A	N/A	N/A	70	25.4	[43]
Sawdust	750	Treatment with monoethanolamine	0.15	N/A	N/A	N/A	30	39.7	[43]
Sawdust	750	Treatment with monoethanolamine	0.15	N/A	N/A	N/A	70	22.6	[43]
Sawdust	850	Unmodified biochar	182.04	N/A	N/A	N/A	30	47.5	[43]
Sawdust	850	Unmodified biochar	182.04	N/A	N/A	N/A	70	28.8	[43]
Sawdust	850	Treatment with monoethanolamine	3.17	N/A	N/A	N/A	30	44.8	[43]
Sawdust	850	Treatment with monoethanolamine	3.17	N/A	N/A	N/A	70	25.2	[43]
Walnut shell	500	Unmodified biochar	94.509	N/A	0.054	0.021	N/A	N/A	[47]
Walnut shell	900	Unmodified biochar	397.015	N/A	0.198	0.159	25 70	72.6 30.07	[47]

1
2
3
4
5
6
7
8
9
10
11
12
13
14
15
16
17
18
19
20
21
22
23
24
25
26
27
28
29
30
31
32
33
34
35
36
37
38
39
40
41
42
43
44
45
46
47
48
49

Feedstock	Pyrolysis temperature (°C)	Modification	BET surface area (m ² /g)	Surface area of micropores (m ² /g)	Total pore volume (cm ³ /g)	Micro pore volume (cm ³ /g)	Adsorption temperature (°C)	CO ₂ adsorption capacity (mg/g)	Reference
Walnut shell	900	Mg loaded	292.002	N/A	0.157	0.118	25 70	82.04 43.76	[47]
Cottonwood	600	Unmodified biochar (CW)	99	N/A	0.01	N/A	25	57.96	[108]
Cottonwood	600	Mg:CW = 0.01	275	N/A	0.01	N/A	25	63.69	[108]
Cottonwood	600	Mg:CW = 0.25	244	N/A	0.03	N/A	25	47.69	[108]
Cottonwood	600	Mg:CW = 1	184	N/A	0.1	N/A	25	35.35	[108]
Cottonwood	600	Mg:CW = 3	228	N/A	0.12	N/A	25	33.83	[108]
Cottonwood	600	Mg:CW = 6	197	N/A	0.29	N/A	25	27.79	[108]
Cottonwood	600	Mg:CW = 20	289	N/A	0.25	N/A	25	35.05	[108]
Cottonwood	600	Mg:CW = 40	262	N/A	0.27	N/A	25	32.33	[108]
Cottonwood	600	Al:CW = 0.025	256	N/A	0.01	N/A	25	63.87	[108]
Cottonwood	600	Al:CW = 0.25	206	N/A	0.03	N/A	25	62.98	[108]
Cottonwood	600	Al:CW = 2.5	331	N/A	0.3	N/A	25	69.3	[108]
Cottonwood	600	Al:CW = 1	263	N/A	0.25	N/A	25	64.63	[108]
Cottonwood	600	Al:CW = 3	370	N/A	0.39	N/A	25	69.49	[108]
Cottonwood	600	Al:CW = 4	367	N/A	0.37	N/A	25	71.05	[108]
Cottonwood	600	Fe:CW = 0.01	302	N/A	0.01	N/A	25	64.3	[108]
Cottonwood	600	Fe:CW = 0.05	NA	N/A	NA	N/A	25	55.61	[108]
Cottonwood	600	Fe:CW = 0.1	458	N/A	0.04	N/A	25	66.57	[108]
Cottonwood	600	Fe:CW = 5	665	N/A	0.59	N/A	25	60.68	[108]
Cottonwood	600	Fe:CW = 6	654	N/A	0.19	N/A	25	65.26	[108]
Cottonwood	600	Fe:CW = 10	749	N/A	0.33	N/A	25	53.79	[108]

4.2 Amino-modified biochar

Ammonia modification or the introduction of basic functional groups such as N-containing functional groups onto biochar surface increases the affinity of biochar for adsorbing acidic CO₂ as a result of the increase in alkalinity. Soybean straw biochar modified with CO₂-NH₃ had a higher CO₂ adsorption capacity (88.89 mg/g) than NH₃-modified (79.19 mg/g) and CO₂-modified (76.31 mg/g) biochar [67]. Contrasting results were observed in a study conducted with cotton stalk biochar produced by fast pyrolysis and modified with CO₂, NH₃, and CO₂ + NH₃ [57]. In that study, CO₂-modified biochar derived from cotton stalk at 800 °C performed better in CO₂ adsorption at 20 °C (99.42 mg/g) than the NH₃ or NH₃ + CO₂-modified biochars because of the better micropore structure [57]. However, the CO₂ adsorption capacity of biochar activated with either NH₃ or NH₃ + CO₂ increased with the increase of activation temperature from 500 °C to 800 °C where as a slight reduction in CO₂ adsorption could be observed in biochar activated with 900 °C compared to that of 800 °C (Table 2). A similar trend could be observed in the micropore surface area of biochar modified with NH₃ and NH₃ + CO₂. When biochar was modified first with CO₂ and followed by NH₃, CO₂ could combine with biochar surface to produce active sites to facilitate introducing N containing functional groups [66]. Nevertheless, introduction of excessive amounts of N functional groups may block the micropore entrance and reduce the surface area [66].

4.3 Carbon dioxide activation of biochar

Gas purging or the modification of biochar with CO₂ is a physical modification method [109],[103],[41]. Several studies have proven that CO₂ activation enhances micropores, which favors CO₂ adsorption [57],[110]. During CO₂ modification, CO₂ reacts with the C of biochar to form CO (known as hot corrosion) and creates a more microporous structure [99].

1
2
3
4
5
6
7
8
9
10
11
12
13
14
15
16
17
18
19
20
21
22
23
24
25
26
27
28
29
30
31
32
33
34
35
36
37
38
39
40
41
42
43
44
45
46
47
48
49
50
51
52
53
54
55
56
57
58
59
60
61
62
63
64
65

492 Moreover, the gas purging facilitates the thermal degradation of carbonaceous material and
493 enhances the aromaticity of the biochar [27],[111]. Studies have revealed that the capacity of
494 CO₂ adsorption in CO₂-modified biochar is significantly higher than that of unmodified
495 biochar [41]. In addition, CO₂-modified biochar has a higher surface area and pore volume
496 than unmodified and NH₃-modified biochar, and CO₂ adsorption capacity shows a significant
497 linear relationship with the micropore volume [41],[57]. Studies have revealed that the CO₂
498 adsorption capacity shows an increasing trend with increasing activation temperature (Table
499 2) [57]. In addition, after CO₂ activation, the synthesized carbon materials are of high purity,
500 and, thus, a washing stage after completion of the activation process is not needed. Therefore,
501 gas purging is more advantageous than chemical activation [112].

502 503 4.4 Steam-activated biochar

504 During steam activation, biochar is subjected to partial gasification with steam, which
505 enhances the devolatilization and the formation of a crystalline structure [99]. The oxygen
506 from water molecules in carbon surface sites, create surface oxides and H₂. Then, the
507 produced H₂ reacts with C surface sites, forming surface hydrogen complexes and activating
508 the biochar surface [99]. Even though CO₂-activated biochar and steam-activated biochar
509 have similar micropore volumes, steam-activated biochar has a higher total pore volume than
510 that of CO₂-activated biochar [107]. Steam-activated carbon has a higher graphitic carbon
511 content and lower oxygen-containing group content than that of KOH-activated carbon [107].
512 However, it was found that the adsorption capacity of steam-activated carbon begins to
513 reduce from the 20th cycle, which indicates that the steam-activated biochar may not be
514 suitable for multicycle CO₂ adsorption [107].

515 516 4.5 Metal-impregnated biochar

1
2
3
4
5
6
7
8
9
10
11
12
13
14
15
16
17
18
19
20
21
22
23
24
25
26
27
28
29
30
31
32
33
34
35
36
37
38
39
40
41
42
43
44
45
46
47
48
49
50
51
52
53
54
55
56
57
58
59
60
61
62
63
64
65

517 Some studies have also used metal oxyhydroxide biochar composites to increase the
518 adsorption capacity of biochar [49]. It has been found that the adsorption of acidic CO₂ can
519 be enhanced by increasing the alkalinity of the biochar surface. Therefore, the introduction of
520 metal groups including Na, Ca, Mg, Al, Ni, and Fe onto the biochar surface will increase
521 basic sites on the surface of biochar, and hence, this method serves as a promising option to
522 improve the CO₂ adsorption capacity of biochar [47]. Lahijani *et al.* [47] reported that a
523 biochar incorporating Mg showed a higher CO₂ adsorption capacity (82.0 mg/g) than that of
524 raw biochar (72.6 mg/g) at 25 °C and 1 atm (Table 2). Moreover, cyclic CO₂ capture studies
525 showed that Mg-loaded biochar has high stability in its CO₂ capture capacity [47]. Generally,
526 metal oxyhydroxides are basic and tend to bond with the CO₂ molecules which are acidic.
527 Therefore, metal oxyhydroxide–biochar composites such as the Fe₂O₃–biochar composite,
528 which has ferromagnetic properties because of the presence of iron oxide, can be used to
529 enhance the CO₂ adsorption capacity of biochar [49]. Even though, the presence of high
530 surface area with abundant adsorption sites are important for high CO₂ adsorption, Creamer
531 *et al* [10] found a poor correlation between the surface area and CO₂ adsorption on biochar
532 modified with aluminium oxide suggesting that presence of large surface area does not
533 always ensure high adsorption. Moreover, interaction between iron oxide and CO₂ particles
534 were significantly weaker than that of AlOOH [10].

535 536 **5. Current challenges facing the practical application of biochar-based adsorbents**

537 Biochar-based adsorbents have been claimed to have advantages of being low-cost,
538 renewable, and suitable for the removal of multiple contaminants (i.e., they can remove
539 chemical, biological, and physical contaminants), and, thus, they have been the subject of
540 extensive studies over the past ten years [113]. However, there are still various challenges

1 541 that prevent the practical, large-scale application of biochar-based adsorbents for CO₂
2 542 removal.
3

4
5 543 First, the robustness and stability of biochar-based adsorbents have not been fully
6
7 544 demonstrated, despite the fact that high adsorption capacities and long-term cyclic operation
8
9 545 are critical to ensure the economics and practicality of the technology [114]. Huang *et al.* [45]
10
11 546 found that the CO₂ adsorption capacity of rice straw biochar produced by microwave
12
13 547 pyrolysis was around 10 mg/g lower than that of activated carbon and suggested that
14
15 548 processes such as activation and impregnation are required to enhance the capacity of the
16
17 549 biochar. Lahijani *et al.* [47] impregnated walnut shell pyrolysis biochar with various types of
18
19 550 metals (Mg, Al, Fe, Ni, Ca, and Na), followed by N₂ heat treatment, and found that the
20
21 551 adsorption capacity increased from 72.6 mg/g for raw biochar to 82.0 mg/g for Mg-loaded
22
23 552 biochar. Nevertheless, the enhanced adsorption is still significantly smaller than that of
24
25 553 conventional activated carbon (e.g., type A-20, type Maxsorb III and phenol-formaldehyde
26
27 554 resin-based), which has an adsorption capacity of several hundreds of milligrams per gram
28
29 555 [115]. It is worth noting that any modification process may add extra costs and carbon
30
31 556 footprint to the biochar-based adsorbents, and these have not been quantified yet.
32
33
34
35
36
37
38

39 557 Secondly, existing experiments are mainly based on simulated gas mixtures that
40
41 558 consist of either pure CO₂ or a simple combination of several gas components (e.g., CO₂, N₂,
42
43 559 and H₂O) [116]. For cases where multiple gaseous agents exist, it is important to know if the
44
45 560 gases other than CO₂ will affect the adsorption capacity of CO₂ (i.e., competitive adsorption),
46
47 561 as well as how the biochar affects the concentrations of these other gases. For example, the
48
49 562 adsorption capacity of CO₂ could be reduced by the H₂O initially adsorbed on the carbon
50
51 563 [116]. Few studies have investigated the use of biochar-based adsorbents to remove CO₂ in
52
53 564 practical, large-scale applications [37]. The composition of actual flue or product gas can be
54
55 565 more complicated than that of the simulated gas. Thus, more studies are required to clarify
56
57
58
59
60
61
62
63
64
65

1 566 the principles and mechanisms underlying the competitive adsorption of biochar in actual flue
2 567 or product gas so that specific biochar-based adsorbents can be developed for certain flue or
3
4 568 product gas compositions. The CO₂ adsorption capacity of biochar in indoor spaces or a
5
6
7 569 specific space can be predicted by airflow simulation programs using computational fluid
8
9
10 570 dynamics (CFD). A 2D mathematical model for CO₂ absorption using CFD was developed
11
12 571 by Hajilary and Rezakazemi [117], and, in their study, the simulation results were compared
13
14 572 with the experimental data, and the effects of the liquid flowrate, different nanoparticles, and
15
16
17 573 nanoparticle concentration on the process efficiency were investigated. Hooff and Blocken
18
19 574 [118] conducted CFD simulation analysis on the natural ventilation of a large semi-enclosed
20
21
22 575 stadium using the CO₂ concentration decay method.

23
24 576 Third, to complete the knowledge loop of the whole CO₂ capture and reuse cycle, it
25
26 577 is also necessary to understand the principles and mechanisms for the regeneration and
27
28
29 578 disposal of biochar. The regeneration ability for reuse of adsorbent after using for CO₂
30
31 579 removal is an important feature for determining the economic efficiency of the adsorbent
32
33
34 580 [39]. Bamdad *et al.* [119] found that the CO₂ adsorption capacity of nitrogen-functionalized
35
36 581 sawmill-residue-based biochar decreased by 4–8% after five cycles and by 20% after 10
37
38
39 582 cycles. Nguyen and Lee [39] showed that the CO₂ adsorption capacity of nitrogen doped
40
41 583 biochar decreased by 15% after 10 cycles. Apart from that, metal oxy-hydroxide biochar
42
43 584 composites produced using aluminium, iron or magnesium demonstrated excellent
44
45
46 585 regeneration capacity ranging from 90-99% at 120 °C [108] which is relatively low
47
48
49 586 regeneration temperature compared to other studies [120]. Activated carbon produced with
50
51 587 KOH or CO₂ activation using biochar also exhibited good regeneration ability up to 50 cycles
52
53
54 588 whereas adsorption capacity of steam activated carbon started to decrease after 20 cycles
55
56 589 suggesting that steam activated carbon is not favorable for multi cyclic adsorption [107].
57
58
59 590 Although they claimed that the regeneration rates were satisfactory, higher rates have been
60
61
62
63
64
65

1
2
3
4
5
6
7
8
9
10
11
12
13
14
15
16
17
18
19
20
21
22
23
24
25
26
27
28
29
30
31
32
33
34
35
36
37
38
39
40
41
42
43
44
45
46
47
48
49
50
51
52
53
54
55
56
57
58
59
60
61
62
63
64
65

591 achieved for other types of CO₂ adsorbents. For example, the CO₂ adsorption capacity of
592 polyHIPE/PEI-based adsorbent only decreased by about 5% after 10 cycles [121], and the
593 adsorption capacity of the APTES-grafted ordered mesoporous silica KIT-6 remained almost
594 constant after 10 cycles [122]. The large loss in CO₂ capture capacity after cyclic adsorption
595 may increase the cost of regeneration and limit the use of biochar as a carbon sequestering
596 material. Alternatively, CO₂-saturated biochar can be used in an admixture to replace some of
597 the cement used in building materials, which would lead to the valorization of biochar at the
598 end of its service life as a CO₂ adsorbent. Gupta *et al.* [123] reported that the addition of 2%
599 saw dust biochar saturated with CO₂ (SatBC) in cement mortar pre-deployment improved the
600 early strength and reduced the water penetration depth compared to the control mortar.
601 Although the 28-day strength and capillary absorption of SatBC was affected by the presence
602 of CO₂ in the biochar pores, this type of biochar can be used in non-structural cement-based
603 materials where strength and durability considerations are less important than those of
604 structural materials [123].

605 Biochar may be contaminated by pollutants (e.g., Volatile Organic Compounds
606 (VOCs), Polycyclic Aromatic Hydrocarbons (PAHs), heavy metals and particulates) during
607 the production process and service life [12],[65],. It has been found that PAHs concentration
608 is greatly influenced by feedstock type and production temperature and resident time. Biochar
609 produced with slow pyrolysis possess low PAH content compared to that of fast pyrolysis
610 possibly due to longer resident time during slow pyrolysis, PAHs may release to the gaseous
611 phase whereas during fast pyrolysis or gasification, PAHs can be concentrated on biochar
612 [124]. Buss *et al.* [125] found that PAH content in biochar produced from straw was 5.8 times
613 higher than that of biochar produced with wood biomass suggesting that lignin content and
614 the composition of lignin in biomass greatly influenced the PAH content in biochar. Apart
615 from that, studies have observed that VOC content in biochar decreased with the increase of

1 616 pyrolysing temperature and whereas gasification resulted in low levels of VOCs compared to
2 617 hydrothermal carbonization [12]. Moreover, if the feedstock is naturally low in heavy metal
3
4 618 content, biochar derived from that feedstock also consist of less amount of heavy metals
5
6
7 619 suggesting that it is a prerequisite to select appropriate feedstock to ensure safe application
8
9
10 620 [126]. Hence, careful selection of clean feedstock and appropriate conversion technology
11
12 621 with proper temperature range and residence time is essential to minimize contaminants in
13
14 622 biochar [12].

16
17 623 Kua *et al.* [127] studied the effect of particulate materials (0.27–22.50 μm) on the
18
19 624 CO_2 adsorption capacity of biochar produced from wood waste at 500 $^\circ\text{C}$ and 10 $^\circ\text{C}/\text{min}$. The
20
21 625 study showed that the deposition of fine particulate material on the surfaces and pores of the
22
23
24 626 biochar can reduce the CO_2 adsorption capacity by 8.33 times in an environment containing
25
26 627 600 ppm CO_2 . However, limited information is available regarding the impact of chemical
27
28
29 628 pollutants on the CO_2 adsorption capacity of biochar and the flue gas composition. The
30
31 629 presence of the pollutants may indirectly affect the disposal of spent biochar, e.g., limiting its
32
33
34 630 use as a soil additive [128],[129]. Indeed, there is limited information regarding the
35
36 631 ecotoxicology and human health risks associated with the use of biochar-based adsorbents
37
38
39 632 [113]. Thus, it is necessary to develop specific standards about the concentrations of the
40
41 633 pollutants in biochar for certain compositions of flue or product gas and for matching with
42
43
44 634 the biochar disposal method.

45
46 635 Fourth, both physical and chemical modification methods have been proposed and
47
48
49 636 tested in laboratory-scale experiments. However, most studies are explorative in nature and
50
51 637 the effectiveness of the methods for large-scale biochar modification and application is still
52
53 638 unclear. The techno-economic and environmental feasibility of the methods for the
54
55
56 639 application of biochar-based adsorbents must be examined from a system and life-cycle
57
58 640 perspective, as has been done for conventional carbon capture and sequestration technologies
59
60
61
62
63
64
65

1
2
3
4
5
6
7
8
9
10
11
12
13
14
15
16
17
18
19
20
21
22
23
24
25
26
27
28
29
30
31
32
33
34
35
641 [130],[131]]. For example, pyrolysis is an endothermic process and requires a sustained
642 external heat source, whose impact on the whole-life-cycle carbon footprint of biochar-based
643 CO₂ adsorption technology remains unclear. As far as possible, life-cycle assessments of
644 biochar production and application systems should be consequential in nature so that the
645 system boundaries (and, thus, the impacts assessed) include the co-products of the pyrolysis
646 or gasification processes. Examples of consequential assessments for slag can be found in
647 Kua et al.[133],[134]. Correspondingly, the optimization and design parameters of practical,
648 large-scale biochar-based CO₂ removal systems are still lacking. In addition, in terms of the
649 indoor environment, it is possible to reduce the concentration of CO₂ in the indoor space by
650 applying biochar to the filter of the ventilation device or the building materials. However,
651 because the physical properties may change during the manufacture of building materials and
652 filters including biochar, a clear test method for building materials must be reviewed. Such
653 studies will shed light on how the price of biochar sorbents can be affected by various factors,
654 such as labor, feedstock, production efficiencies [135], and even the pricing of the co-
655 products.

36
37
38
39
40
41
42
43
44
45
46
47
48
49
50
51
52
53
54
55
56
57
58
59
60
61
62
63
64
65
656 Finally, it is desirable to develop a systematic database containing information
657 ranging from the selection of suitable (cost, properties, or availability) feedstocks,
658 physicochemical properties of biochar products, methods and effects of biochar upgrading,
659 impacts of the presence of multiple gas agents, recovery of adsorbed CO₂, and regeneration
660 and disposal of biochar, along with the relevant cost-benefit and environmental information.
661 The database will serve as the basis for making an informed decision about the practical use
662 of biochar-based adsorbents for CO₂ removal. The development of a databank of biochar-
663 based adsorbents necessitates consistent or standardized experiment designs and data
664 reporting, which do not currently exist.

666 **6. Conclusions**

667 Biochar is a potential cost-effective and sustainable material for CO₂ adsorption
668 because of its inherent properties. However, the surface area, micropore area, micropore
669 volume, presence of basic functional groups and hetero atoms play vital roles in the CO₂
670 adsorption capacity of biochar. Thus, the modification of biochar through chemical and
671 physical processes to enhance the surface characteristics will significantly improve the CO₂
672 adsorption capacity of biochar. However, few studies have been performed with respect to
673 the large-scale production and use of modified biochar for capturing CO₂. Hence, further
674 studies should focus on the development of novel technologies and biochar composites such
675 as metal organic framework (MOF) and carbon-based nanomaterials to enhance the CO₂
676 adsorption capacity of biochar. Moreover, the field-scale application of biochar for CO₂
677 adsorption should also be a focus in the future, as well as the development of new
678 technologies for the regeneration and reuse of captured CO₂ or its conversion into useable
679 products.

681 **Acknowledgment**

682 This study was supported by the Korea Ministry of Environment (MOE) as "Technology
683 Program for establishing biocide safety management" (2018002490001) and Hydrogen
684 Energy Innovation Technology Development Program of the National Research Foundation
685 of Korea (NRF) funded by the Korean government (Ministry of Science and ICT(MSIT))
686 (NRF-2019M3E6A1064197).

687 **References**

- 688 [1] Liu C, Yao Z, Wang K, Zheng X, Li B. Net ecosystem carbon and greenhouse gas
689 budgets in fiber and cereal cropping systems. *Sci Total Environ* 2019;647:895–904.
690 doi:10.1016/j.scitotenv.2018.08.048.

- 691 [2] Marescaux A, Thieu V, Garnier J. Carbon dioxide, methane and nitrous oxide
1 692 emissions from the human-impacted Seine watershed in France. *Sci Total Environ*
2 693 2018;643:247–59. doi:10.1016/j.scitotenv.2018.06.151.
- 3 694 [3] IPCC, 2014: Climate Change 2014: Impacts, Adaptation, and Vulnerability. Part B:
4 695 Regional Aspects. Contribution of Working Group II to the Fifth Assessment Report
5 696 of the Intergovernmental Panel on Climate Change [Barros, V.R., C.B. Field, D.J.
6 697 Dokken, M.D pp. 688. IPCC, 2014: Climate Change 2014: Impacts, Adaptation, and
7 698 Vulnerability. Part B: Regional Aspects. Contribution of Working Group II to the Fifth
8 699 Assessment Report of the Intergovernmental Panel on Climate Change [Barros, V.R.,
9 700 C.B. Field, D.J. Dokken, M.D. *Ippc* 2014:688. doi:10.1007/s13398-014-0173-7.2.
- 11 701 [4] Dutcher B, Fan M, Russell AG. Amine-based CO₂ capture technology development
12 702 from the beginning of 2013-A review. *ACS Appl Mater Interfaces* 2015;7:2137–48.
13 703 doi:10.1021/am507465f.
- 14 704 [5] Guo T, Ma N, Pan Y, Bedane AH, Xiao H, Eić M, et al. Characteristics of
15 705 CO₂ adsorption on biochar derived from biomass pyrolysis in molten salt.
16 706 *Can J Chem Eng* 2018;9999:1–9. doi:10.1002/cjce.23153.
- 17 707 [6] Zhao H, Luo X, Zhang H, Sun N, Wei W, Sun Y. Carbon-based adsorbents for post-
18 708 combustion capture: a review. *Greenh Gases Sci Technol* 2018;8:11–36.
19 709 doi:10.1002/ghg.1758.
- 20 710 [7] González AS, Plaza MG, Rubiera F, Pevida C. Sustainable biomass-based carbon
21 711 adsorbents for post-combustion CO₂ capture. *Chem Eng J* 2013;230:456–65.
22 712 doi:10.1016/j.cej.2013.06.118.
- 23 713 [8] Yaumi AL, Bakar MZA, Hameed BH. Recent advances in functionalized composite
24 714 solid materials for carbon dioxide capture. *Energy* 2017;124:461–80.
25 715 doi:10.1016/j.energy.2017.02.053.
- 26 716 [9] Shafeeyan MS, Daud WMAW, Houshmand A, Shamiri A. A review on surface
27 717 modification of activated carbon for carbon dioxide adsorption. *J Anal Appl Pyrolysis*
28 718 2010;89:143–51. doi:10.1016/j.jaap.2010.07.006.
- 29 719 [10] Creamer AE, Gao B. Carbon-Based Adsorbents for Postcombustion CO₂ Capture: A
30 720 Critical Review. *Environ Sci Technol* 2016;50:7276–89. doi:10.1021/acs.est.6b00627.
- 31 721 [11] Shao J, Zhang J, Zhang X, Feng Y, Zhang H, Zhang S, et al. Enhance SO₂ adsorption
32 722 performance of biochar modified by CO₂ activation and amine impregnation. *Fuel*
33 723 2018;224:138–46. doi:10.1016/j.fuel.2018.03.064.
- 34 724 [12] Ok, Y.S., Tsang, D.C., Bolan, N. and Novak, J.M. (Eds.) 2018. *Biochar from Biomass*
35 725 *and Waste: Fundamentals and Applications*. Elsevier. ISBN: 9780128117309
- 36 726 [13] Zhang X, Gao B, Creamer AE, Cao C, Li Y. Adsorption of VOCs onto engineered
37 727 carbon materials: A review. *J Hazard Mater* 2017;338:102–23.
38 728 doi:10.1016/j.jhazmat.2017.05.013.
- 39 729 [14] Liu WJ, Jiang H, Yu HQ. Development of Biochar-Based Functional Materials:
40 730 Toward a Sustainable Platform Carbon Material. *Chem Rev* 2015;115:12251–85.
41 731 doi:10.1021/acs.chemrev.5b00195.
- 42 732 [15] El-Naggar A, Lee SS, Awad YM, Yang X, Ryu C, Rizwan M, et al. Influence of soil
43 733 properties and feedstocks on biochar potential for carbon mineralization and
44 734 improvement of infertile soils. *Geoderma* 2018;332:100–8.
45 735 doi:10.1016/j.geoderma.2018.06.017.
- 46 736 [16] Ahmad M, Lee SS, Lee SE, Al-Wabel MI, Tsang DCW, Ok YS. Biochar-induced
47 737 changes in soil properties affected immobilization/mobilization of metals/metalloids in
48 738 contaminated soils. *J Soils Sediments* 2017;17:717–30. doi:10.1007/s11368-015-1339-
49 739 4.

- 740 [17] Beiyuan J, Awad YM, Beckers F, Tsang DCW, Ok YS, Rinklebe J. Mobility and
1 741 phytoavailability of As and Pb in a contaminated soil using pine sawdust biochar under
2 742 systematic change of redox conditions. *Chemosphere* 2017;178:110–8.
3 743 doi:10.1016/j.chemosphere.2017.03.022.
- 4 744 [18] Ahmad M, Rajapaksha AU, Lim JE, Zhang M, Bolan N, Mohan D, et al. Biochar as a
5 745 sorbent for contaminant management in soil and water: a review. *Chemosphere*
6 746 2014;99:19–33. doi:10.1016/j.chemosphere.2013.10.071.
- 7 747 [19] Woolf D, Amonette JE, Street-Perrott FA, Lehmann J, Joseph S. Sustainable biochar
8 748 to mitigate global climate change. *Nat Commun* 2010;1:1–9.
9 749 doi:10.1038/ncomms1053.
- 10 750 [20] Xiong X, Yu IKM, Cao L, Tsang DCW, Zhang S, Ok YS. A review of biochar-based
11 751 catalysts for chemical synthesis, biofuel production, and pollution control. *Bioresour*
12 752 *Technol* 2017;246:254–70. doi:10.1016/j.biortech.2017.06.163.
- 13 753 [21] You S, Ok YS, Tsang DCW, Kwon EE, Wang H, You S, et al. Towards practical
14 754 application of gasification : A critical review from syngas and biochar perspec-
15 755 tives. *Crit Rev Environ Sci Technol* 2017;0:1–48. doi:10.1080/10643389.2018.1518860.
- 16 756 [22] Qian K, Kumar A, Zhang H, Bellmer D, Huhnke R. Recent advances in utilization of
17 757 biochar. *Renew Sustain Energy Rev* 2015;42:1055–64. doi:10.1016/j.rser.2014.10.074.
- 18 758 [23] Inyang MI, Gao B, Yao Y, Xue Y, Zimmerman A, Mosa A, et al. Technology A
19 759 review of biochar as a low-cost adsorbent for aqueous heavy metal removal. *Crit Rev*
20 760 *Environ Sci Technol* 2016;46:406–33. doi:10.1080/10643389.2015.1096880.
- 21 761 [24] Rajapaksha AU, Ok YS, El-Naggar A, Kim H, Song F, Kang S, et al. Dissolved
22 762 organic matter characterization of biochars produced from different feedstock
23 763 materials. *J Environ Manage* 2019;233:393–9. doi:10.1016/j.jenvman.2018.12.069.
- 24 764 [25] He X, Liu Z, Niu W, Yang L, Zhou T, Qin D, et al. Effects of pyrolysis temperature on
25 765 the physicochemical properties of gas and biochar obtained from pyrolysis of crop
26 766 residues. *Energy* 2018;143:746–56. doi:10.1016/j.energy.2017.11.062.
- 27 767 [26] Yang X, Yu IKM, Cho D-W, Chen SS, Tsang DCW, Shang J, et al. Tin-
28 768 Functionalized Wood Biochar as a Sustainable Solid Catalyst for Glucose
29 769 Isomerization in Biorefinery. *ACS Sustain Chem Eng*
30 770 2019;7:acssuschemeng.8b05311. doi:10.1021/acssuschemeng.8b05311.
- 31 771 [27] Yang X, Tsibart A, Nam H, Hur J, El-Naggar A, Tack FMG, et al. Effect of
32 772 gasification biochar application on soil quality: Trace metal behavior, microbial
33 773 community, and soil dissolved organic matter. *J Hazard Mater* 2019;365:684–94.
34 774 doi:10.1016/j.jhazmat.2018.11.042.
- 35 775 [28] Ashiq A, Adassooriya NM, Sarkar B, Rajapaksha AU, Ok YS, Vithanage M.
36 776 Municipal solid waste biochar-bentonite composite for the removal of antibiotic
37 777 ciprofloxacin from aqueous media. *J Environ Manage* 2019;236:428–35.
38 778 doi:10.1016/j.jenvman.2019.02.006.
- 39 779 [29] Melo TM, Bottlinger M, Schulz E, Leandro WM, Menezes de Aguiar Filho A, Wang
40 780 H, et al. Plant and soil responses to hydrothermally converted sewage sludge
41 781 (sewchar). *Chemosphere* 2018;206:338–48. doi:10.1016/j.chemosphere.2018.04.178.
- 42 782 [30] Li Y, Ruan G, Jalilov AS, Tarkunde YR, Fei H, Tour JM. Biochar as a renewable
43 783 source for high-performance CO₂ sorbent. *Carbon N Y* 2016;107:344–51.
44 784 doi:10.1016/j.carbon.2016.06.010.
- 45 785 [31] Huang H, Tang J, Gao K, He R, Zhao H, Werner D. Characterization of KOH
46 786 modified biochars from different pyrolysis temperatures and enhanced adsorption of
47 787 antibiotics. *RSC Adv* 2017;7:14640–8. doi:10.1039/c6ra27881g.
- 48 788 [32] Sophia A. C, Lima EC. Removal of emerging contaminants from the environment by
49 789 adsorption. *Ecotoxicol Environ Saf* 2018;150:1–17. doi:10.1016/j.ecoenv.2017.12.026.

- 790 [33] Xu X, Schierz A, Xu N, Cao X. Comparison of the characteristics and mechanisms of
1 791 Hg(II) sorption by biochars and activated carbon. *J Colloid Interface Sci* 2016;463:55–
2 792 60. doi:10.1016/j.jcis.2015.10.003.
- 3 793 [34] Alhashimi HA, Aktas CB. Life cycle environmental and economic performance of
4 794 biochar compared with activated carbon: A meta-analysis. *Resour Conserv Recycl*
5 795 2017;118:13–26.
- 6 796 [35] Lehmann J, Roberts KG, Gloy BA, Joseph S, Scott NR. Life cycle assessment of
7 797 biochar systems: Estimating the energetic, economic, and climate change potential.
8 798 *Environ Sci Technol* 2010;44:827–33. doi:10.1021/es902266r.
- 9 799 [36] Rajapaksha AU, Chen SS, Tsang DCW, Zhang M, Vithanage M, Mandal S, et al.
10 800 Engineered/designer biochar for contaminant removal/immobilization from soil and
11 801 water: Potential and implication of biochar modification. *Chemosphere* 2016;148:276–
12 802 91. doi:10.1016/j.chemosphere.2016.01.043.
- 13 803 [37] Wang B, Gao B, Fang J. Recent advances in engineered biochar productions and
14 804 applications. *Crit Rev Environ Sci Technol* 2017;47:2158–207.
15 805 doi:10.1080/10643389.2017.1418580.
- 16 806 [38] Chatterjee R, Sajjadi B, Mattern DL, Chen WY, Zubatiuk T, Leszczynska D, et al.
17 807 Ultrasound cavitation intensified amine functionalization: A feasible strategy for
18 808 enhancing CO₂ capture capacity of biochar. *Fuel* 2018;225:287–98.
19 809 doi:10.1016/j.fuel.2018.03.145.
- 20 810 [39] Nguyen MV, Lee BK. A novel removal of CO₂ using nitrogen doped biochar beads as
21 811 a green adsorbent. *Process Saf Environ Prot* 2016;104:490–8.
22 812 doi:10.1016/j.psep.2016.04.007.
- 23 813 [40] Zhang X, Zhang S, Yang H, Feng Y, Chen Y, Wang X, et al. Nitrogen enriched
24 814 biochar modified by high temperature CO₂-ammonia treatment: Characterization and
25 815 adsorption of CO₂. *Chem Eng J* 2014;257:20–7. doi:10.1016/j.cej.2014.07.024.
- 26 816 [41] Xiong Z, Shihong Z, Haiping Y, Tao S, Yingquan C, Hanping C. Influence of
27 817 NH₃/CO₂ Modification on the Characteristic of Biochar and the CO₂ Capture.
28 818 *Bioenergy Res* 2013;6:1147–53. doi:10.1007/s12155-013-9304-9.
- 29 819 [42] Azlina W, Ab W, Ghani K, Rebitanim NZ, Amran M, Salleh M, et al. Carbon Dioxide
30 820 Adsorption on Coconut Shell Biochar n.d.;1:683–93. doi:10.1007/978-3-319-16709-1.
- 31 821 [43] Madzaki H, Karimghani WAWAB, Nurzalikharebitanim, Azilbaharialias. Carbon
32 822 Dioxide Adsorption on Sawdust Biochar. *Procedia Eng* 2016;148:718–25.
33 823 doi:10.1016/j.proeng.2016.06.591.
- 34 824 [44] Liu SH, Huang YY. Valorization of coffee grounds to biochar-derived adsorbents for
35 825 CO₂ adsorption. *J Clean Prod* 2018;175:354–60. doi:10.1016/j.jclepro.2017.12.076.
- 36 826 [45] Huang YF, Chiueh P Te, Shih CH, Lo SL, Sun L, Zhong Y, et al. Microwave pyrolysis
37 827 of rice straw to produce biochar as an adsorbent for CO₂ capture. *Energy* 2015;84:75–
38 828 82. doi:10.1016/j.energy.2015.02.026.
- 39 829 [46] Xu X, Kan Y, Zhao L, Cao X. Chemical transformation of CO₂ during its capture by
40 830 waste biomass derived biochars. *Environ Pollut* 2016;213:533–40.
41 831 doi:10.1016/j.envpol.2016.03.013.
- 42 832 [47] Lahijani P, Mohammadi M, Mohamed AR. Metal incorporated biochar as a potential
43 833 adsorbent for high capacity CO₂ capture at ambient condition. *J CO₂ Util*
44 834 2018;26:281–93. doi:10.1016/j.jcou.2018.05.018.
- 45 835 [48] Creamer AE, Gao B, Zhang M. Carbon dioxide capture using biochar produced from
46 836 sugarcane bagasse and hickory wood. *Chem Eng J* 2014;249:174–9.
47 837 doi:10.1016/j.cej.2014.03.105.

- 838 [49] Creamer AE, Gao B, Wang S. Carbon dioxide capture using various metal
1 839 oxyhydroxide-biochar composites. *Chem Eng J* 2016;283:826–32.
2 840 doi:10.1016/j.cej.2015.08.037.
- 3 841 [50] Plaza MG, González AS, Pis JJ, Rubiera F, Pevida C. Production of microporous
4 842 biochars by single-step oxidation: Effect of activation conditions on CO₂ capture.
5 843 *Appl Energy* 2014;114:551–62. doi:10.1016/j.apenergy.2013.09.058.
- 6 844 [51] Sethupathi S, Zhang M, Rajapaksha AU, Lee SR, Nor NM, Mohamed AR, et al.
7 845 Biochars as potential adsorbers of CH₄, CO₂ and H₂S. *Sustain* 2017;9:1–10.
8 846 doi:10.3390/su9010121.
- 9 847 [52] Post-combustion CO₂ capture with a commercial activated carbon: comparison of
10 848 different regeneration strategies M.G. Plaza, S. García, F. Rubiera, J.J. Pis, C. Pevida*
11 849 Instituto Nacional del Carbón, CSIC, Apartado 73, 33080 Oviedo, Spain n.d.:1–28.
- 12 850 [53] Gargiulo V, Gomis-Berenguer A, Giudicianni P, Ania CO, Ragucci R, Alfe M.
13 851 Assessing the potential of bio-chars prepared by steam assisted slow pyrolysis for CO₂
14 852 adsorption and separation. *Energy and Fuels* 2018.
15 853 doi:10.1021/acs.energyfuels.8b01058.
- 16 854 [54] Chiang Y, Juang R. Journal of the Taiwan Institute of Chemical Engineers Surface
17 855 modifications of carbonaceous materials for carbon dioxide adsorption : A review. *J*
18 856 *Taiwan Inst Chem Eng* 2017;71:214–34. doi:10.1016/j.jtice.2016.12.014.
- 19 857 [55] Liu Y, Lonappan L, Brar SK, Yang S. Impact of biochar amendment in agricultural
20 858 soils on the sorption, desorption, and degradation of pesticides: A review. *Sci Total*
21 859 *Environ* 2018;645:60–70. doi:10.1016/j.scitotenv.2018.07.099.
- 22 860 [56] Sun Y, Gao B, Yao Y, Fang J, Zhang M, Zhou Y, et al. Effects of feedstock type ,
23 861 production method , and pyrolysis temperature on biochar and hydrochar properties.
24 862 *Chem Eng J* 2014;240:574–8. doi:10.1016/j.cej.2013.10.081.
- 25 863 [57] Zhang X, Zhang S, Yang H, Feng Y, Chen Y, Wang X, et al. Nitrogen enriched
26 864 biochar modified by high temperature CO₂-ammonia treatment: Characterization and
27 865 adsorption of CO₂. *Chem Eng J* 2014;257:20–7. doi:10.1016/j.cej.2014.07.024.
- 28 866 [58] Igalavithana AD, Lee SE, Lee YH, Tsang DCW, Rinklebe J, Kwon EE, et al. Heavy
29 867 metal immobilization and microbial community abundance by vegetable waste and
30 868 pine cone biochar of agricultural soils. *Chemosphere* 2017;174:593–603.
31 869 doi:10.1016/j.chemosphere.2017.01.148.
- 32 870 [59] Kim KH, Kim JY, Cho TS, Choi JW. Influence of pyrolysis temperature on
33 871 physicochemical properties of biochar obtained from the fast pyrolysis of pitch pine
34 872 (*Pinus rigida*). *Bioresour Technol* 2012;118:158–62.
35 873 doi:10.1016/j.biortech.2012.04.094.
- 36 874 [60] Shaaban A, Se SM, Dimin MF, Juoi JM, Mohd Husin MH, Mitan NMM. Influence of
37 875 heating temperature and holding time on biochars derived from rubber wood sawdust
38 876 via slow pyrolysis. *J Anal Appl Pyrolysis* 2014;107:31–9.
39 877 doi:10.1016/j.jaap.2014.01.021.
- 40 878 [61] Gai X, Wang H, Liu J, Zhai L, Liu S, Ren T, et al. Effects of feedstock and pyrolysis
41 879 temperature on biochar adsorption of ammonium and nitrate. *PLoS One* 2014;9:1–19.
42 880 doi:10.1371/journal.pone.0113888.
- 43 881 [62] Ng WC, You S, Ling R, Gin KYH, Dai Y, Wang CH. Co-gasification of woody
44 882 biomass and chicken manure: Syngas production, biochar reutilization, and cost-
45 883 benefit analysis. *Energy* 2017;139:732–42. doi:10.1016/j.energy.2017.07.165.
- 46 884 [63] Zhang J, Huang B, Chen L, Li Y, Li W, Luo Z. Characteristics of biochar produced
47 885 from yak manure at different pyrolysis temperatures and its effects on the yield and
48 886 growth of highland barley. *Chem Speciat Bioavailab* 2018;00:1–11.
49 887 doi:10.1080/09542299.2018.1487774.
- 50
51
52
53
54
55
56
57
58
59
60
61
62
63
64
65

- 888 [64] Liu Y, Yao S, Wang Y, Lu H, Brar SK, Yang S. Bio- and hydrochars from rice straw
1 889 and pig manure: Inter-comparison. *Bioresour Technol* 2017;235:332–7.
2 890 doi:10.1016/j.biortech.2017.03.103.
- 3 891 [65] You S, Ok YS, Chen SS, Tsang DCW, Kwon EE, Lee J, et al. A critical review on
4 892 sustainable biochar system through gasification: Energy and environmental
5 893 applications. *Bioresour Technol* 2017;246:242–53.
6 894 doi:10.1016/j.biortech.2017.06.177.
- 7 895 [66] Zhang X, Zhang S, Yang H, Feng Y, Chen Y, Wang X, et al. Nitrogen enriched
8 896 biochar modified by high temperature CO₂-ammonia treatment: Characterization and
9 897 adsorption of CO₂. *Chem Eng J* 2014;257:20–7. doi:10.1016/j.cej.2014.07.024.
- 10 898 [67] Zhang X, Wu J, Yang H, Shao J, Wang X, Chen Y, et al. Preparation of nitrogen-
11 899 doped microporous modified biochar by high temperature CO₂-NH₃treatment for
12 900 CO₂adsorption: Effects of temperature. *RSC Adv* 2016;6:98157–66.
13 901 doi:10.1039/c6ra23748g.
- 14 902 [68] Palansooriya KN, Wong JTF, Hashimoto Y, Huang L, Rinklebe J, Chang SX, et al.
15 903 Response of microbial communities to biochar-amended soils: a critical review.
16 904 *Biochar* 2019;1:3–22. doi:10.1007/s42773-019-00009-2.
- 17 905 [69] Hansen V, Müller-Stöver D, Ahrenfeldt J, Holm JK, Henriksen UB, Hauggaard-
18 906 Nielsen H. Gasification biochar as a valuable by-product for carbon sequestration and
19 907 soil amendment. *Biomass and Bioenergy* 2015;72:300–8.
20 908 doi:10.1016/j.biombioe.2014.10.013.
- 21 909 [70] Chen B, Zhou D, Zhu L. Transitional adsorption and partition of nonpolar and polar
22 910 aromatic contaminants by biochars of pine needles with different pyrolytic
23 911 temperatures. *Environ Sci Technol* 2008;42:5137–43. doi:10.1021/es8002684.
- 24 912 [71] Yang X, Igalavithana AD, Oh SE, Nam H, Zhang M, Wang CH, et al. Characterization
25 913 of bioenergy biochar and its utilization for metal/metalloid immobilization in
26 914 contaminated soil. *Sci Total Environ* 2018;640–641:704–13.
27 915 doi:10.1016/j.scitotenv.2018.05.298.
- 28 916 [72] Mayakaduwa SS, Herath I, Ok YS, Mohan D, Vithanage M. Insights into aqueous
29 917 carbofuran removal by modified and non-modified rice husk biochars. *Environ Sci*
30 918 *Pollut Res* 2017;24:22755–63. doi:10.1007/s11356-016-7430-6.
- 31 919 [73] Sun Y, Gao B, Yao Y, Fang J, Zhang M, Zhou Y, et al. Effects of feedstock type,
32 920 production method, and pyrolysis temperature on biochar and hydrochar properties.
33 921 *Chem Eng J* 2014;240:574–8. doi:10.1016/j.cej.2013.10.081.
- 34 922 [74] Sigmund G, Bucheli TD, Hilber I, Micić V, Kah M, Hofmann T. Effect of ageing on
35 923 the properties and polycyclic aromatic hydrocarbon composition of biochar. *Environ*
36 924 *Sci Process Impacts* 2017;19:768–74. doi:10.1039/c7em00116a.
- 37 925 [75] Wang S, Gao B, Zimmerman AR, Li Y, Ma L, Harris WG, et al. Physicochemical and
38 926 sorptive properties of biochars derived from woody and herbaceous biomass.
39 927 *Chemosphere* 2015;134:257–62. doi:10.1016/j.chemosphere.2015.04.062.
- 40 928 [76] Cao X, Harris W. Properties of dairy-manure-derived biochar pertinent to its potential
41 929 use in remediation. *Bioresour Technol* 2010;101:5222–8.
42 930 doi:10.1016/j.biortech.2010.02.052.
- 43 931 [77] Cantrell KB, Hunt PG, Uchimiya M, Novak JM, Ro KS. Impact of pyrolysis
44 932 temperature and manure source on physicochemical characteristics of biochar.
45 933 *Bioresour Technol* 2012;107:419–28. doi:10.1016/j.biortech.2011.11.084.
- 46 934 [78] Lee J, Yang X, Cho SH, Kim JK, Lee SS, Tsang DCW, et al. Pyrolysis process of
47 935 agricultural waste using CO₂for waste management, energy recovery, and biochar
48 936 fabrication. *Appl Energy* 2017;185:214–22. doi:10.1016/j.apenergy.2016.10.092.

- 937 [79] Pacioni TR, Soares D, Domenico M Di, Rosa MF, Moreira R de FPM, José HJ. Bio-
1 938 syngas production from agro-industrial biomass residues by steam gasification. *Waste*
2 939 *Manag* 2016;58:221–9. doi:10.1016/j.wasman.2016.08.021.
- 3 940 [80] Zhang Z, Zhou J, Xing W, Xue Q, Yan Z, Zhuo S, et al. Critical role of small
4 941 micropores in high CO₂ uptake. *Phys Chem Chem Phys* 2013;15:2523.
5 942 doi:10.1039/c2cp44436d.
- 6 943 [81] Sevilla M, Fuertes AB. CO₂adsorption by activated templated carbons. *J Colloid*
7 944 *Interface Sci* 2012;366:147–54. doi:10.1016/j.jcis.2011.09.038.
- 8 945 [82] Chiang YC, Juang RS. Surface modifications of carbonaceous materials for carbon
9 946 dioxide adsorption: A review. *J Taiwan Inst Chem Eng* 2017;71:214–34.
10 947 doi:10.1016/j.jtice.2016.12.014.
- 11 948 [83] Angin D. Effect of pyrolysis temperature and heating rate on biochar obtained from
12 949 pyrolysis of safflower seed press cake. *Bioresour Technol* 2013;128:593–7.
13 950 doi:10.1016/j.biortech.2012.10.150.
- 14 951 [84] Zhang Z, Zhou J, Xing W, Xue Q, Yan Z, Zhuo S, et al. Critical role of small
15 952 micropores in high CO₂ uptake. *Phys Chem Chem Phys* 2013;15:2523.
16 953 doi:10.1039/c2cp44436d.
- 17 954 [85] Shafeeyan MS, Daud WMAW, Houshmand A, Shamiri A. A review on surface
18 955 modification of activated carbon for carbon dioxide adsorption. *J Anal Appl Pyrolysis*
19 956 2010;89:143–51. doi:10.1016/j.jaap.2010.07.006.
- 20 957 [86] Shen W, Fan W. Nitrogen-containing porous carbons: Synthesis and application. *J*
21 958 *Mater Chem A* 2013;1:999–1013. doi:10.1039/c2ta00028h.
- 22 959 [87] Xing W, Liu C, Zhou Z, Zhou J, Wang G, Zhuo S, et al. Oxygen-containing functional
23 960 group-facilitated CO₂capture by carbide-derived carbons. *Nanoscale Res Lett*
24 961 2014;9:1–8. doi:10.1186/1556-276X-9-189.
- 25 962 [88] Liu Y, Wilcox J. Effects of surface heterogeneity on the adsorption of CO₂ in
26 963 microporous carbons. *Environ Sci Technol* 2012;46:1940–7. doi:10.1021/es204071g.
- 27 964 [89] Shahkarami S, Dalai AK, Soltan J. Enhanced CO₂ Adsorption Using MgO-
28 965 Impregnated Activated Carbon: Impact of Preparation Techniques. *Ind Eng Chem Res*
29 966 2016;55:5955–64. doi:10.1021/acs.iecr.5b04824.
- 30 967 [90] Nugent P, Giannopoulou EG, Burd SD, Elemento O, Giannopoulou EG, Forrest K, et
31 968 al. Porous materials with optimal adsorption thermodynamics and kinetics for
32 969 CO₂separation. *Nature* 2013;495:80–4. doi:10.1038/nature11893.
- 33 970 [91] Gao F, Li Y, Bian Z, Hu J, Liu H. Dynamic hydrophobic hindrance effect of
34 971 zeolite@zeolitic imidazolate framework composites for CO₂capture in the presence of
35 972 water. *J Mater Chem A* 2015;3:8091–7. doi:10.1039/c4ta06645f.
- 36 973 [92] Shen Y, Linville JL, Ignacio-de Leon PAA, Schoene RP, Urgun-Demirtas M. Towards
37 974 a sustainable paradigm of waste-to-energy process: Enhanced anaerobic digestion of
38 975 sludge with woody biochar. *J Clean Prod* 2016;135:1054–64.
39 976 doi:10.1016/j.jclepro.2016.06.144.
- 40 977 [93] Keiluweit M, Nico PS, Johnson MG. Dynamic Molecular Structure of Plant Biomass-
41 978 Derived Black Carbon (Biochar). *Environ Sci Technol* 2010;44:1247–53.
- 42 979 [94] Igalavithana AD, Mandal S, Niazi NK, Vithanage M, Parikh SJ, Mukome FND, et al.
43 980 Advances and future directions of biochar characterization methods and applications.
44 981 *Crit Rev Environ Sci Technol* 2017;47:2275–330.
45 982 doi:10.1080/10643389.2017.1421844.
- 46 983 [95] Regmi P, Garcia Moscoso JL, Kumar S, Cao X, Mao J, Schafran G. Removal of
47 984 copper and cadmium from aqueous solution using switchgrass biochar produced via
48 985 hydrothermal carbonization process. *J Environ Manage* 2012;109:61–9.
49 986 doi:10.1016/j.jenvman.2012.04.047.

- 987 [96] Ok YS, Chang SX, Gao B, Chung HJ. SMART biochar technology-A shifting
1 988 paradigm towards advanced materials and healthcare research. *Environ Technol Innov*
2 989 2015;4:206–9. doi:10.1016/j.eti.2015.08.003.
- 3 990 [97] Igalavithana AD, Mandal S, Niazi NK, Vithanage M, Parikh SJ, Mukome FND, et al.
4 991 Advances and future directions of biochar characterization methods and applications.
5 992 *Crit Rev Environ Sci Technol* 2017;47:2275–330.
6 993 doi:10.1080/10643389.2017.1421844.
- 7 994 [98] Yao Y, Gao B, Fang J, Zhang M, Chen H, Zhou Y, et al. Characterization and
8 995 environmental applications of clay-biochar composites. *Chem Eng J* 2014;242:136–43.
9 996 doi:10.1016/j.cej.2013.12.062.
- 10 997 [99] Upamali A, Chen SS, Tsang DCW, Zhang M, Vithanage M, Mandal S, et al.
11 998 Chemosphere Engineered / designer biochar for contaminant removal / immobilization
12 999 from soil and water : Potential and implication of biochar modification. *Chemosphere*
13 1000 2016;148:276–91. doi:10.1016/j.chemosphere.2016.01.043.
- 14 1001 [100] Fan Y, Wang B, Yuan S, Wu X, Chen J, Wang L. Adsorptive removal of
15 1002 chloramphenicol from wastewater by NaOH modified bamboo charcoal. *Bioresour*
16 1003 *Technol* 2010;101:7661–4. doi:10.1016/j.biortech.2010.04.046.
- 17 1004 [101] Li J, Lv G, Bai W, Liu Q, Zhang Y, Song J. Modification and use of biochar from
18 1005 wheat straw (*Triticum aestivum* L.) for nitrate and phosphate removal from water.
19 1006 *Desalin Water Treat* 2014;57:1–13. doi:10.1080/19443994.2014.994104.
- 20 1007 [102] Basta AH, Fierro V, El-Saied H, Celzard A. 2-Steps KOH activation of rice straw: An
21 1008 efficient method for preparing high-performance activated carbons. *Bioresour Technol*
22 1009 2009;100:3941–7. doi:10.1016/j.biortech.2009.02.028.
- 23 1010 [103] Bhatnagar A, Hogland W, Marques M, Sillanpää M. An overview of the modification
24 1011 methods of activated carbon for its water treatment applications. *Chem Eng J*
25 1012 2013;219:499–511. doi:10.1016/j.cej.2012.12.038.
- 26 1013 [104] Otowa T, Nojima Y, Miyazaki T. Development of KOH activated high surface area
27 1014 carbon and its application to drinking water purification. *Carbon N Y* 1997;35:1315–9.
28 1015 doi:10.1016/S0008-6223(97)00076-6.
- 29 1016 [105] Mao H, Zhou D, Hashisho Z, Wang S, Chen H, Wang H. Preparation of pinewood-
30 1017 and wheat straw-based activated carbon via a microwave-assisted potassium hydroxide
31 1018 treatment and an analysis of the effects of the microwave activation conditions.
32 1019 *BioResources* 2015;10:809–21. doi:10.15376/biores.10.1.809-821.
- 33 1020 [106] Jang E, Choi SW, Hong SM, Shin S, Lee KB. Development of a cost-effective
34 1021 CO₂adsorbent from petroleum coke via KOH activation. *Appl Surf Sci* 2018;429:62–
35 1022 71. doi:10.1016/j.apsusc.2017.08.075.
- 36 1023 [107] Shahkarami S, Azargohar R, Dalai AK, Soltan J. Breakthrough CO₂ adsorption in
37 1024 bio-based activated carbons. *J Environ Sci (China)* 2015;34:68–76.
38 1025 doi:10.1016/j.jes.2015.03.008.
- 39 1026 [108] Creamer AE, Gao B, Wang S. Carbon dioxide capture using various metal
40 1027 oxyhydroxide – biochar composites. *Chem Eng J* 2016;283:826–32.
41 1028 doi:10.1016/j.cej.2015.08.037.
- 42 1029 [109] Guo S, Peng J, Li W, Yang K, Zhang L, Zhang S, et al. Effects of CO₂activation on
43 1030 porous structures of coconut shell-based activated carbons. *Appl Surf Sci*
44 1031 2009;255:8443–9. doi:10.1016/j.apsusc.2009.05.150.
- 45 1032 [110] Rashidi NA, Yusup S. An overview of activated carbons utilization for the post-
46 1033 combustion carbon dioxide capture. *J CO₂ Util* 2016;13:1–16.
47 1034 doi:10.1016/j.jcou.2015.11.002.
- 48 1035 [111] Igalavithana AD, Yang X, Zahra HR, Tack FMG, Tsang DCW, Kwon EE, et al.
49 1036 Metal(loid) immobilization in soils with biochars pyrolyzed in N₂ and CO₂

- 1037 environments. *Sci Total Environ* 2018;630:1103–14.
 1 1038 doi:10.1016/j.scitotenv.2018.02.185.
- 2 1039 [112] Rashidi NA, Yusup S. An overview of activated carbons utilization for the post-
 3 1040 combustion carbon dioxide capture. *Biochem Pharmacol* 2016;13:1–16.
 4 1041 doi:10.1016/j.jcou.2015.11.002.
- 5 1042 [113] Gwenzi W, Chaukura N, Noubactep C, Mukome FND. Biochar-based water treatment
 6 1043 systems as a potential low-cost and sustainable technology for clean water provision. *J*
 7 1044 *Environ Manage* 2017;197:732–49. doi:10.1016/j.jenvman.2017.03.087.
- 8 1045 [114] Han Y, Cao X, Ouyang X, Sohi SP, Chen J. Adsorption kinetics of magnetic biochar
 9 1046 derived from peanut hull on removal of Cr (VI) from aqueous solution: Effects of
 10 1047 production conditions and particle size. *Chemosphere* 2016;145:336–41.
 11 1048 doi:10.1016/j.chemosphere.2015.11.050.
- 12 1049 [115] Singh VK, Anil Kumar E. Measurement and analysis of adsorption isotherms of
 13 1050 CO₂ on activated carbon. *Appl Therm Eng* 2016;97:77–86.
 14 1051 doi:10.1016/j.applthermaleng.2015.10.052.
- 15 1052 [116] Plaza MG, Durán I, Querejeta N, Rubiera F, Pevida C. Experimental and Simulation
 16 1053 Study of Adsorption in Postcombustion Conditions Using a Microporous Biochar. 1.
 17 1054 CO₂ and N₂ Adsorption. *Ind Eng Chem Res* 2016;55:3097–112.
 18 1055 doi:10.1021/acs.iecr.5b04856.
- 19 1056 [117] Hajilary N, Rezakazemi M. CFD modeling of CO₂ capture by water-based nanofluids
 20 1057 using hollow fiber membrane contactor. *Int J Greenh Gas Control* 2018;77:88–95.
 21 1058 doi:10.1016/j.ijggc.2018.08.002.
- 22 1059 [118] Van Hooff T, Blocken B. CFD evaluation of natural ventilation of indoor
 23 1060 environments by the concentration decay method: CO₂ gas dispersion from a semi-
 24 1061 enclosed stadium. *Build Environ* 2013;61:1–17. doi:10.1016/j.buildenv.2012.11.021.
- 25 1062 [119] Bamdad H, Hawboldt K, MacQuarrie S. Nitrogen Functionalized Biochar as a
 26 1063 Renewable Adsorbent for Efficient CO₂ Removal. *Energy & Fuels* 2018;32:11742–8.
 27 1064 doi:10.1021/acs.energyfuels.8b03056.
- 28 1065 [120] Ghanbari S, Kamath G. Dynamic simulation and mass transfer study of carbon dioxide
 29 1066 capture using biochar and MgO impregnated activated carbon in a swing adsorption
 30 1067 process. *Energy & Fuels* 2019;33:acs.energyfuels.9b00923.
 31 1068 doi:10.1021/acs.energyfuels.9b00923.
- 32 1069 [121] Irani M, Jacobson AT, Gasem KAM, Fan M. Facilely synthesized porous polymer as
 33 1070 support of poly(ethyleneimine) for effective CO₂ capture. *Energy* 2018;157:1–9.
 34 1071 doi:10.1016/j.energy.2018.05.141.
- 35 1072 [122] Kishor R, Ghoshal AK. APTES grafted ordered mesoporous silica KIT-6 for
 36 1073 CO₂ adsorption. *Chem Eng J* 2015;262:882–90. doi:10.1016/j.cej.2014.10.039.
- 37 1074 [123] Gupta S, Kua HW, Low CY. Use of biochar as carbon sequestering additive in cement
 38 1075 mortar. *Cem Concr Compos* 2018;87:110–29.
 39 1076 doi:10.1016/j.cemconcomp.2017.12.009.
- 40 1077 [124] Hilber I, Mayer P, Gouliarmou V, Hale SE, Cornelissen G, Schmidt HP, et al.
 41 1078 Bioavailability and bioaccessibility of polycyclic aromatic hydrocarbons from (post-
 42 1079 pyrolytically treated) biochars. *Chemosphere* 2017;174:700–7.
 43 1080 doi:10.1016/j.chemosphere.2017.02.014.
- 44 1081 [125] Buss W, Graham MC, MacKinnon G, Mašek O. Strategies for producing biochars with
 45 1082 minimum PAH contamination. *J Anal Appl Pyrolysis* 2016;119:24–30.
 46 1083 doi:10.1016/j.jaap.2016.04.001.
- 47 1084 [126] Yang X, Ng W, Wong BSE, Baeg GH, Wang CH, Ok YS. Characterization and
 48 1085 ecotoxicological investigation of biochar produced via slow pyrolysis: Effect of

1086 feedstock composition and pyrolysis conditions. *J Hazard Mater* 2019;365:178–85.
 1 1087 doi:10.1016/j.jhazmat.2018.10.047.

2 1088 [127] Kua H, Pedapati C, Lee R, Production SK-J of C, 2018 undefined. Effect of indoor
 3 1089 contamination on carbon dioxide adsorption of wood-based biochar—lessons for direct
 4 1090 air capture. *Elsevier* 2019;210:860–71. doi:10.1016/j.jclepro.2018.10.206.

5 1091 [128] Dutta T, Kwon E, Bhattacharya SS, Jeon BH, Deep A, Uchimiya M, et al. Polycyclic
 6 1092 aromatic hydrocarbons and volatile organic compounds in biochar and biochar-
 7 1093 amended soil: a review. *GCB Bioenergy* 2017;9:990–1004. doi:10.1111/gcbb.12363.

8 1094 [129] Hilber I, Bastos AC, Loureiro S, Soja G, Marsz A, Cornelissen G, et al. The different
 9 1095 faces of biochar: contamination risk versus remediation tool. *J Environ Eng Landsc
 10 1096 Manag* 2017;25:86–104. doi:10.3846/16486897.2016.1254089.

11 1097 [130] Parker L, Folger P, Stine DD. Capturing CO from coal-fired power plants: Challenges
 12 1098 for a comprehensive strategy. *CRS Rep Congr* 2008.

13 1099 [131] Smebye AB, Sparrevik M, Schmidt HP, Cornelissen G. Life-cycle assessment of
 14 1100 biochar production systems in tropical rural areas: Comparing flame curtain kilns to
 15 1101 other production methods. *Biomass and Bioenergy* 2017;101:35–43.
 16 1102 doi:10.1016/j.biombioe.2017.04.001.

17 1103 [132] Groesbeck JG, Pearce JM. Coal with Carbon Capture and Sequestration is not as Land
 18 1104 Use Efficient as Solar Photovoltaic Technology for Climate Neutral Electricity
 19 1105 Production. *Sci Rep* 2018;8. doi:10.1038/s41598-018-31505-3.

20 1106 [133] Kua HW. Integrated policies to promote sustainable use of steel slag for construction -
 21 1107 A consequential life cycle embodied energy and greenhouse gas emission perspective.
 22 1108 *Energy Build* 2015;101:133–43. doi:10.1016/j.enbuild.2015.04.036.

23 1109 [134] Kua HW. The consequences of substituting sand with used copper slag in construction:
 24 1110 An embodied energy and global warming potential analysis using life cycle approach
 25 1111 and different allocation methods kua life cycle assessment of copper slag. *J Ind Ecol*
 26 1112 2013;17:869–79. doi:10.1111/jiec.12059.

27 1113 [135] Gupta S, Wei H, Dai S. Biochar-mortar composite : Manufacturing , evaluation of
 28 1114 physical properties and economic viability. *Constr Build Mater* 2018;167:874–89.
 29 1115 doi:10.1016/j.conbuildmat.2018.02.104.

30 1116

31 1117

32

33

34

35

36

37

38

39

40

41

42

43

44

45

46

47

48

49

50

51

52

53

54

55

56

57

58

59

60

61

62

63

64

65